*Revised Manuscript
Click here to view linked References

https://doi.org/10.1016/j.ejmech.2019.02.014

This is the Pre-Published Version.

Design, synthesis, and biological evaluation of truncated deguelin derivatives as Hsp90 inhibitors

Hong Yao[a], Feijie Xu[a], Guangyu Wang[a], Shaowen Xie[a],Wenlong Li[a], Hequan Yao[a], Cong Ma[b], Zheying Zhu[c], Jinyi Xu[a,*], and Shengtao Xu[a,*]

[a]State Key Laboratory of Natural Medicines and Department of Medicinal Chemistry, China Pharmaceutical University, 24 Tong Jia Xiang, Nanjing 210009, P. R. China

[b]State Key Laboratory of Chemical Biology and Drug Discovery, and Department of Applied Biology and Chemical Technology, The Hong Kong Polytechnic University, Kowloon, Hong Kong

[c]Division of Molecular Therapeutics & Formulation, School of Pharmacy, The University of Nottingham, University Park Campus, Nottingham NG7 2RD, U.K.

***Correspondence should be addressed to:**

Biology: S.T. Xu (cpuxst@cpu.edu.cn)

Chemistry: J.Y. Xu (jinyixu@china.com)

Abstract:

A series of novel B- and C-rings truncated deguelin derivatives have been designed and synthesized in the present study as heat shock protein 90 (Hsp90) inhibitors. The synthesized compounds exhibited micromolar antiproliferative potency toward a panel of human cancer cell lines. Their structure-activity relationships (SARs) were investigated in a systematic manner. Compound **21c** was identified to have high Hsp90 binding potency (60 nM) and caused degradation of client proteins through ubiquitin proteasome system. Further biological studies showed that compound **21c** induced a dose-dependent S and G2-phase cell cycle arrest on human breast cancer MCF-7 cells. Flow cytometry and Western blot analyses confirmed that compound **21c** caused apoptosis of MCF-7 cells. In addition, compound **21c** showed much potent inhibition on the migration and invasion of MCF-7 cells. Taken together, these results suggest that **21c** might be a promising lead compound for further development of

© 2019. This manuscript version is made available under the CC-BY-NC-ND 4.0 license https://creativecommons.org/licenses/by-nc-nd/4.0/.

Hsp90 inhibitors.

Keywords: Heat shock protein 90; deguelin; structure simplification; anticancer

1. Introduction

Heat shock protein 90 (Hsp90) is attracting increasing attention as a promising target for cancer treatment in recent years[1]. As a constitutively expressed chaperon, Hsp90 plays a central role in assembly, folding, trafficking, and degradation processes of various client proteins involved in pathways of cell proliferation, angiogenesis, invasion and metastasis, and many of them are oncogenic proteins[2]. Additionally, Hsp90 is often overexpressed 2-10 fold higher in cancer cells than that in normal healthy cells[3]. Inhibition of Hsp90 by small molecules would result in degradation of the client proteins and suppress the growth and proliferation of cancers[4].Besides, targeting Hsp90 results in the regulation of multiple pathways simultaneously, and may also overcome the notorious cancer resistance issue due to its potential for combinatorial targeting of multiple oncogenic protein pathways[5]. These properties of Hsp90 make it an ideal and selective target for the treatment of cancers.

Over the past decades, a number of Hsp90 inhibitors have been reported. The earlier Hsp90 inhibitors are developed from natural products, such as geldanamycin (**1**) and radicicol (**2**), which are good lead compounds for the development of Hsp90 inhibitors[6]. 17-AAG (**3**), a semi-synthetic geldanamycin analogue designed to improve activity and reduce toxicity, once progressed to phase II clinical trials to treat patients with metastatic melanoma [7]. Then, various totally synthesized inhibitors of Hsp90 were developed with the aid of structure based drug design strategy[8]. To date, approximately more than 20 different compounds are in clinical studies, however, none Hsp90 inhibitors have been approved for use in clinical[9]. Several clinical trials of Hsp90 inhibitors have been discontinued due to effectiveness and toxicity. Consequently, there is an urgent need to develop new Hsp90 inhibitors.

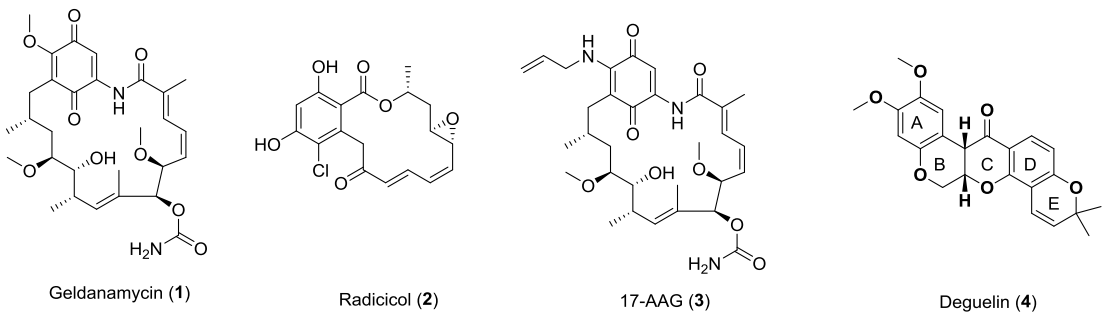

Figure 1. Chemical structures of some Hsp90 inhibitors.

Deguelin (**4**), a rotenoid isolated from the African plant *Mundulea sericea* (Leguminosae) and other plants, has been reported as a Hsp90 inhibitor with potent apoptotic and antiangiogenic effects on transformed cells and a variety of cancer cells[10]. Mechanism studies revealed that deguelin competes with ATP for binding with Hsp90, leading to the decrease of a series of Hsp90 client proteins, including p53, CDK4, MAPK-1/2, Akt, and HIF-1*α*[11]. Despite of promising anticancer activity of deguelin, the potential toxicity (Parkinson's disease-like syndrome) of this compound in rats impended its direct application in clinic[12]. The complex structure of deguelin containing 5-fused rings designated as A-E rings (Figure 1), also raised a challenge for their chemical synthesis for structural modifications[13].

Tuning the structure of natural products plays an important role in transforming natural products to drugs[14]. For some natural products with structurally complex frameworks, truncating the structure may lead to simpler and synthetically more accessible fragment-like scaffolds. These core structures feature from NPs can also be used for further exploration of small druggable molecules[15]. Ring-truncated scaffolds of deguelin have been reported previously[16], however, the detailed structure-activity relationships of truncated deguelin derivatives have not been investigated intensively. In this study, twenty four structurally simpler truncated deguelin derivatives were designed as Hsp90 inhibitors by truncating B- and C-rings from deguelin and further modifying the A-, D- and E-rings (Figure 2). According to the previous reports, presence of the B- and C-rings of deguelin restricted the flexibility of deguelin, limiting the best conformation with which the deguelin

interacted with Hsp90[17]. Our molecular docking study also implied the conformational restriction of deguelin when docking into the active site of Hsp90 (Figure 4B). Besides, the chemical construction of B- and C-rings of deguelin is the hardest step in total synthesis of this natural compound, truncating B- and C-rings of deguelin would be in favorable of chemical synthesis to develop its derivatives as Hsp90 inhibitors [18].

According to the previous studies, the chromene skeleton (D and E rings) of deguelin was important for its activity, and the more extensive changes is inappropriate. Because the previous work implied that the methoxyl group was important to the activity of degelin. The modifications at R2 and carbonyl group were performed to explore the SAR of substitutes of different size and length.

In this work, concise synthetic methodologies were further developed to prepare the novel B- and C-rings truncated deguelin derivatives based on our previous studies [19]. The antiproliferative activities of the synthesized compounds were evaluated and the mechanism of the most potent compound **21c** was also investigated.

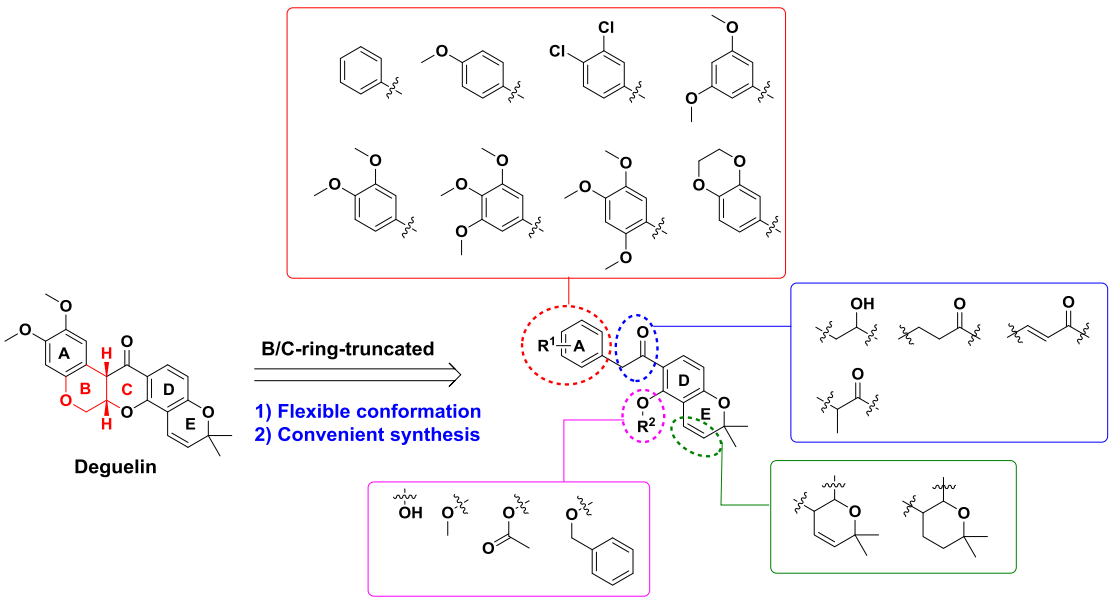

Figure 2. Design strategy of truncated derivatives of deguelin.

2. Results and discussion

2.1. Chemistry

As shown in Scheme 1, the B- and C-rings truncated deguelin derivatives bearing phenolic hydroxy group at chromene moiety were synthesized via Friedel-Crafts acylation in three steps, which was much more concise than previously reported routes[12]. Briefly, acylates **7** were synthesized via Friedel-Crafts acylation using various substituted phenylacetic acids or phenylpropionic acid and resorcinol as starting materials with boron trifluoride diethyl etherate as the solvent. Chromene skeleton was constructed via selective propargylation of resorcinol **7** with 3-chloro-3-methyl-1-butyne and a subsequent regioselective Claisen rearrangement. Thus, truncated deguelin derivatives **9a-f** were obtained in three steps with acceptable total yields.

Scheme 1. Synthesis of truncated deguelin derivatives **9a-f**[a]

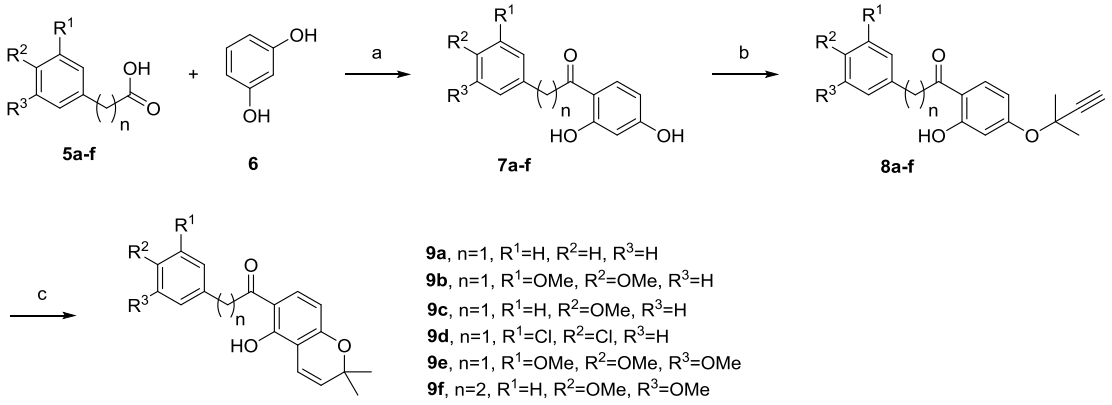

[a]Reagents and conditions: (a) BF_3•Et_2O, N_2, 90°C, 80-90%; (b) 3-Chloro-3-methyl-1-butyne, KI, CuI, K_2CO_3, CH_3CN, rt, 60-75%; (c) *N*,*N*-Dimethylaniline, 150 °C, 85-95%.

With **9a-c** as starting materials, target compounds bearing substitutions of different sizes (methyl, acetyl, and benzyl) at phenolic hydroxy group were obtained. As shown in Scheme 2, in the presence of 1 equiv of methyl iodide, the phenolic hydroxyl group of **9a-c** was methylated preferentially to afford target compounds **10a**, **10c**, and **11**, respectively. However, in the presence of more than 2 equiv of methyl iodide, the α position of carbonyl group was also methylated and gave compounds **10b** and **10d**. The double bond of 2*H*-chromene **11** was reduced in H_2 atmosphere to provide chroman**12** with a 95% yield. On the other hand, the carbonyl group of **11** was

converted to hydroxyl group using $NaBH_4$ as the reductant, affording compound **13**. The following elimination of hydroxyl at 60 ^oC region-selectively provided *trans*-alkenyl compound **14** in 90% yield. Acetylation of compound **9b** with anhydride afforded compound **15**, while benzylation of compound **9b** with excessive benzyl bromide gave dibenzylated compound **16**.

Scheme 2. Synthesis of truncated deguelin derivatives **10**-**16**[a]

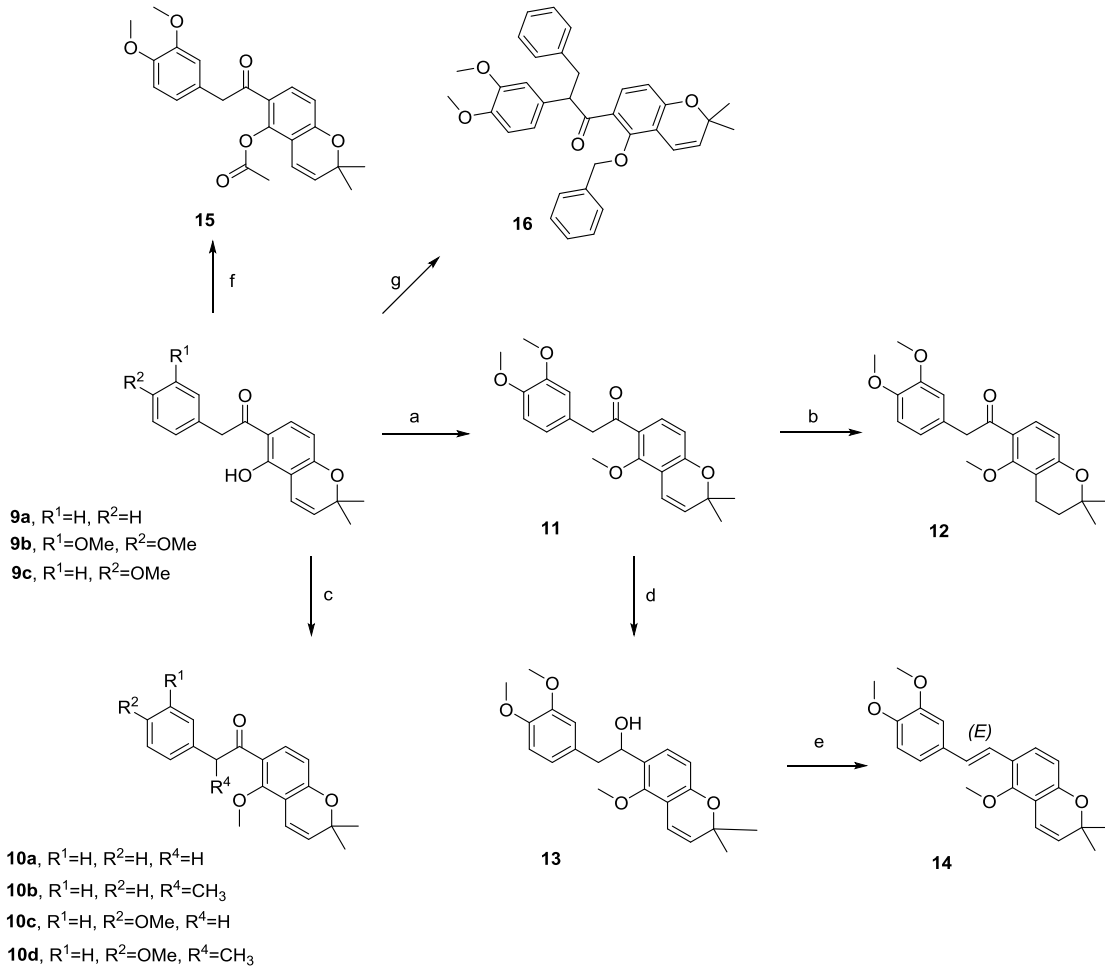

[a]Reagents and conditions: (a) CH_3I (1 equiv.), acetone, reflux, 80%; (b) H_2, Pd/C, MeOH, 95%;(c) CH_3I (2-3 equiv.), acetone, reflux, 80%; (d) $NaBH_4$, MeOH, 0^oC, 95%; (e) AcOH, 60^oC,90%; (f) $(CH_3CO)_2O$, Et_3N, DCM, rt, 90%; (g) BnBr, K_2CO_3, MeCN, reflux, 80%.

Although the preparation of these truncated deguelin derivatives using Friedel-Crafts acylation is very effective, some target compounds could not be

obtained with this methodology due to the lack of commercially available polysubstituted phenylacetic acids. As shown in Scheme 3, key intermediate acylchromene **20** was firstly synthesized from dihydroxyacetophenone (**17**) using the Claisen rearrangement described above. Subsequently compound **20** reacted with various substituted bromobenzene to afford target compounds **21a-e** in moderate yields. Synthesis of chroman **22** from chromene **21d** was accomplished in 95% yield by reduction with H_2 using Pd/C as a catalyst. The aldol condensation of ketone **19** and benzaldehydes under the condition of NaH as base catalyst, THF as solvent provided target compounds **23a-b** in moderate yield.

Scheme 3. Synthesis of truncated deguelin derivatives **21-23**[a]

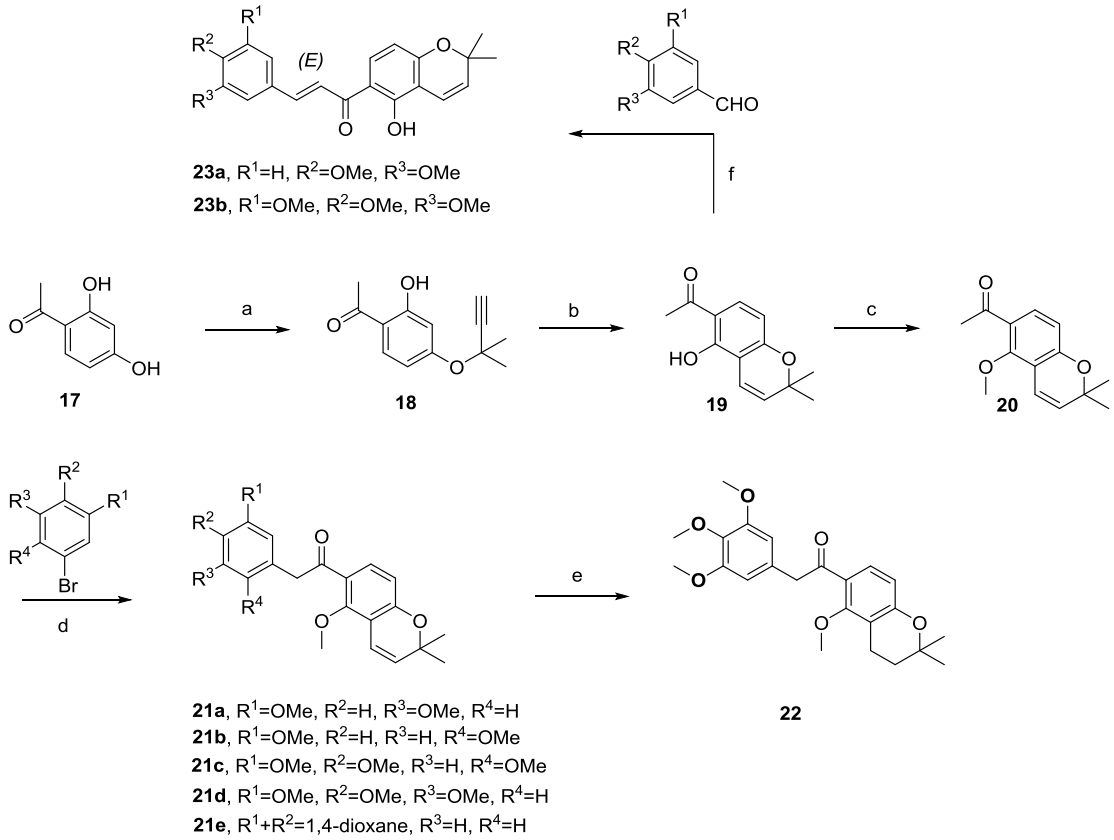

[a]Reagents and conditions: (a) 3-Chloro-3-methyl-1-butyne, KI, CuI, K_2CO_3, CH_3CN, rt, 60%; (b) *N*,*N*-Dimethylaniline,150^{o}C, 95%; (c) CH_3I, acetone, reflux, 80%; (d) $Pd_2(dba)_3$, DPE-phos, *t*-BuOK, THF, 70^{o}C, 70%; (e) H_2, Pd/C, MeOH, 95%; (f) NaH, THF, rt, 65%.

2.2. In vitro antiproliferative activities of truncated deguelin derivatives

All compounds were firstly evaluated for their preliminary antiproliferative activities against human non-small cell lung cancer H1299 cells. Deguelin and Hsp90 inhibitor AT13387 were used as the positive controls. As shown in Table 1, the number and position of methoxy group in A-ring was vital to the antiproliferative effects of these compounds. Replacement of methoxy groups (**9b**) with chlorine atoms (**9d**) reduced the inhibition rate significantly at 10 μM. The inhibition rates of compounds **9a**, **9c**, **9b**, and **9e** increased gradually along with the increase of methoxy groups at A-ring. Trimethoxybenzene seems to be the most favorable moiety for this region (**9e**, **21c**, **21d**, and **22**). Modifications on the linker between A- and D-ring was unfavorable for improving the activity of these derivatives, both increasing the length and reducing carbonyl resulted in analogues with less potent activity. By comparing the inhibition rates at 10 μM between **9c-e** and **10c**, **11**, **21d**, a conclusion could be draw that hydroxyl and methoxyl were all tolerated at D-ring, but large substitutions at D-ring decreased the activity significantly (**15** and **16**). In addition, reducing the double bond of E-ring resulted in increased activity (**12** and **22**).Furthermore, compounds **9e**, **11**, **12**, **21c-d** and **22**, which exhibited potent antiproliferative activities in preliminary screening, were selected for IC_{50} evaluations against H1299, MCF-7 and A549 cell lines. As shown in Table 2, all these compounds exhibited comparable antiproliferative activities to deguelin against three cancer cell lines. Among these compounds, **21c** with a 2,4,5-trimethoxybenzene group was the most potent one with an IC_{50} value of 2.51 μM on MCF-7 cells.

Table 1. Inhibition rates of compounds in H1299 cell line

Compounds	Inhibition rate (%)[a]		
	0.1 μM	1.0 μM	10.0 μM
9a	3.9±1.9	7.8±1.3	15.1±3.8
9b	4.8±2.9	8.2±1.6	45.3±4.2
9c	6.1±1.8	7.1±2.8	16.1±1.9

9d	8.3±2.7	9.1±2.3	11.5±2.3
9e	9.7±2.4	19.7±1.7	49.0±6.5
9f	3.6±0.9	8.5±0.8	30.1±4.8
10a	5.6±1.2	9.3±1.3	11.3±1.8
10b	4.5±1.8	6.5±1.2	15.5±2.0
10c	3.6±0.4	7.3±1.8	10.6±1.5
10d	7.1±1.0	10.8±1.3	13.3±1.9
11	5.1±1.4	10.7±1.4	47.3±4.9
12	7.2±1.5	12.4±1.4	49.3±5.3
13	6.5±0.7	10.8±2.0	19.8±2.0
14	5.2±2.0	8.6±1.8	14.4±1.7
15	4.1±2.0	6.2±0.6	19.5±2.6
16	2.1±1.2	2.5±0.8	9.9±0.8
21a	7.1±1.9	10.2±2.8	40.1±4.7
21b	4.7±1.2	10.4±1.2	38.2±4.3
21c	15.3±1.8	40.3±7.8	72.1±8.0
21d	9.6±1.7	27.4±2.6	58.3±4.8
21e	3.5±0.7	6.5±1.0	28.1±3.9
22	11.0±1.3	30.6±4.3	67.5±4.9
23a	5.3±0.8	6.4±2.1	10.7±2.0
23b	3.8±0.2	8.7±2.1	12.3±1.5
Deguelin	9.9±1.6	28.5±2.7	65.3±7.9
AT13387[b]	94.78±10.6	96.8±7.3	95.7±9.2

[a]Each data represents mean±SD of three independent experiments

[b]Hsp90 inhibitor AT13387 was used as the positive control

Table 2. Hsp90 binding activity and cell antiproliferative effects of representative compounds.

Compounds	IC_{50} (μM)[a]

	H1299	MCF-7	A549	Binding Hsp90 (FP)[b]
9e	12.03±0.95	11.18±0.63	13.05±1.14	0.43
11	11.83±0.96	6.88±0.72	6.00±0.53	0.09
12	12.61±1.12	7.86±0.84	7.20±0.92	0.15
21c	3.40±0.51	2.51±0.28	3.46±0.33	0.06
21d	7.20±0.87	5.08±0.34	6.15±0.71	0.63
22	5.72±0.67	5.22±0.48	5.33±0.57	0.28
Deguelin	5.67±0.35	8.17±0.68	6.05±0.59	1.63
AT13387[c]	0.37±0.06	0.29±0.08	0.44±0.03	0.02

[a]MTT methods, cells were incubated with indicated compounds for 72h, the values are the means of three independent experiments;

[b]Binding to N-terminal domain of Hsp90 was determined by a fluorescence polarization (FP) assay;

[c]Hsp90 inhibitor AT13387 was used as the positive control.

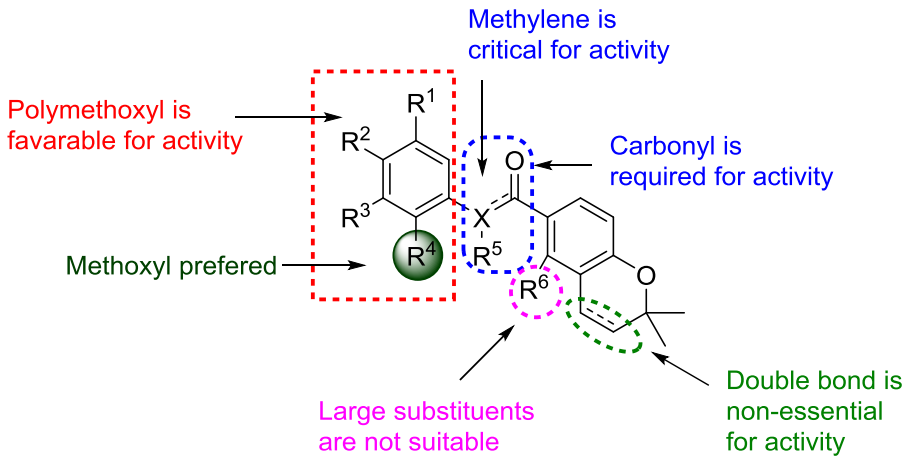

Figure 3. Structure activity relationships of novel anti-tubulin compounds.

*2.3.Compound **21c** directly bound to Hsp90*

In order to confirm whether these compounds could bind to Hsp90, a fluorescence polarization (FP) assay was performed firstly. As shown in Table 2, all the tested target compounds (**9e**, **11**, **12**, **21c**, **21d**, and **22**) showed appreciable binding affinity (0.06-0.43 μM) to recombinant human Hsp90α protein, which were relatively less potent to reference compound AT13387 (0.02 μM), but possessed much higher binding affinity to Hsp90 than deguelin (1.63 μM). Although compound **21c** showed comparable affinity (0.06 μM) to Hsp90 than AT13387 (0.02 μM), the IC_{50} values of **21c** (2.51-3.46 μM) were much higher than that of AT13387 (0.29-0.44 μM) against three cancer cell lines. Besides, the structural similarity of compounds **11** and **21c** resulted similar binding affinity to Hsp90 (0.09 μM for **11** and 0.06 μM for **21c**), but the cytotoxicity of compound **11** was much lower than compound **21c**, we presumed that the reason of this inconsistence might be complex system in a cell.

Next, a monoclonal antibody that specifically bound to Hsp90 was used to immunoprecipitate Hsp90 and then detected whether **21c** could interfere with this process. The results showed that **21c** blocked the binding of Hsp90 with its antibody in a dose-dependent manner (data not shown). In order to understand the more precise binding mode of compound **21c** with Hsp90, docking simulations were performed using the complex between the N-terminal domain of Hsp90 and **21c** (PDB code:5J2X) as a template. The active site of the Hsp90 N-terminal was divided into S1, S2, and S3 three pockets, and deguelin only occupied S1 and S3 pockets (Figure 4A). In addition, there was over contact between deguelin and S3 pocket due to conformational restriction (Figure 4B, deguelin shown in cyan). Truncating B- and C-rings of deguelin relieved the conformational restriction, as shown in Figure 4B, the most potent compound **21c** (shown in pink) was inserted deeply into the S2 pocket and occupied S1, S2, and S3 pockets simultaneously. Interestingly, the SARs of these truncated deguelin derivatives summarized above can be well explained by the binding pattern taken by **21c** in Figure 4D. One methoxyl at A-ring and carbonyl group formed hydrogen bonds to the residue LYS58, oriented the trimethoxybenzene moiety to occupy S2 pocket. The trimethoxybenzene group also formed a pi-cation

interaction with residue LYS58. Excessive size of substitutions at phenolic hydroxyl group of D-ring led to larger shifts, resulting in loss of the key hydrogen bond to the residue LYS58. Taken together, these results suggested that compound **21c** could bind to Hsp90 directly, and this may provide useful information for further design of novel truncated deguelin Hsp90 inhibitors.

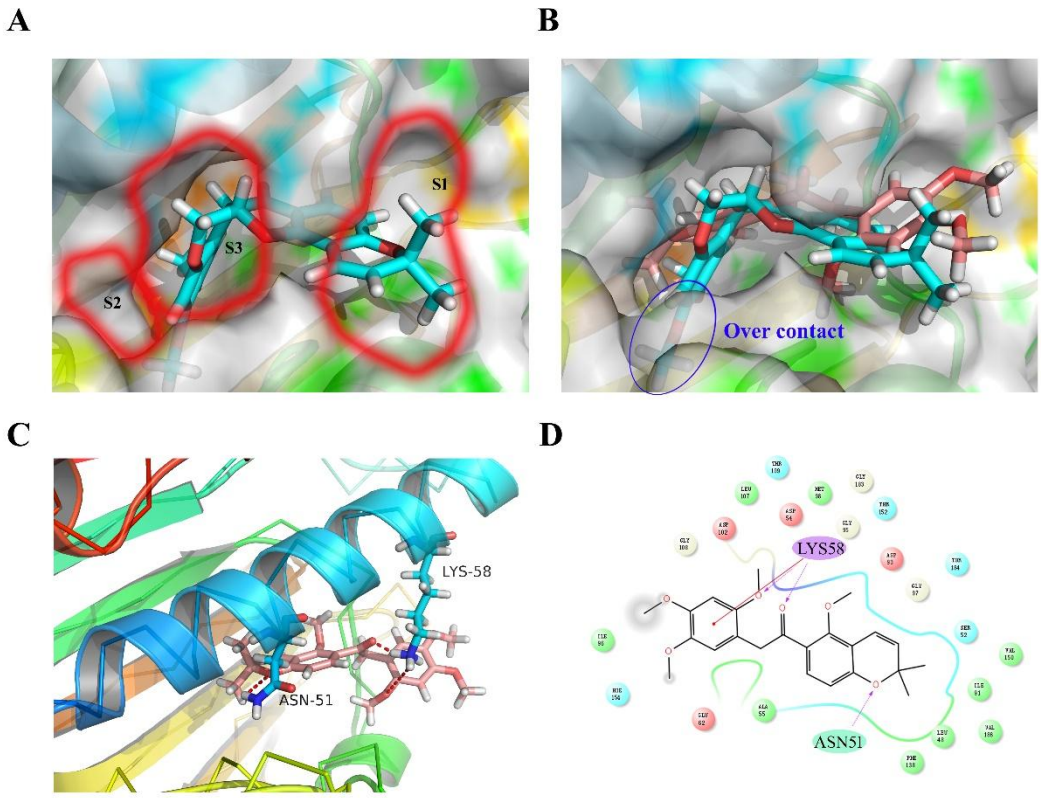

Figure 4. Molecular modeling analysis of deguelin and compound **21c**. (A) The predicted binding model of deguelin to Hsp90 (PDB code: 5J2X) catalytic site. The carbon atoms of deguelin are shown in cyan. The active site of the Hsp90 N-terminal is divided into S1, S2, and S3 three pockets, and deguelin occupies S1 and S3 pockets. (B) Docking poses of deguelin and **21c** with Hsp90. The carbon atoms of deguelin are shown in cyan and the carbon atoms of **21c** are shown in pink. Deguelin has over contact to S3 pocket due to conformational restriction. (C) Docking pose of compound **21c**, key amino acid residues within the binding site are rendered in cyan capped stick. Red dashed lines are hydrogen bonding interactions. (D) The 2D interaction diagram of **21c.** Hydrogen bonds were shown as violet lines and pi-cation interaction is indicated as magenta line.

*2.4. Compound **21c** induced the degradation of Hsp90 client proteins.*

Hsp90 inhibitors often cause rapid decline in client protein activities, and the degradation of client proteins through ubiquitin proteasome system[20]. Protein kinase B (PKB, also known as Akt) is the client protein of Hsp90, in order to investigate whether compound **21c** could decrease the bind of Akt to Hsp90 and increase the ubiquitin-mediated degradation of Akt, co-immunoprecipitate (Co-IP) assay was performed. As shown in Figure 5A, the binding of Akt to Hsp90 could be clearly detected through Co-IP, however, in MCF-7 cells treated with 4 μM **21c**, a decline in Hsp90-binded Akt was observed. Further detection of ubiquinated Akt in **21c** treated cells confirmed that **21c** could bind to Hsp90 and mediate the degradation of Hsp90 client proteins through ubiquitin proteasome system (Figure 5B). Further Western blotting assay was performed to identify the inhibitory profile of **21c** on Hsp90 client proteins. The results showed that **21c** significantly downregulated the levels of Hsp90 clients p-mTOR, p-MAPK, p-AKT, HIF-1α, and survivin in a dose-dependent manner (Figure 5c).

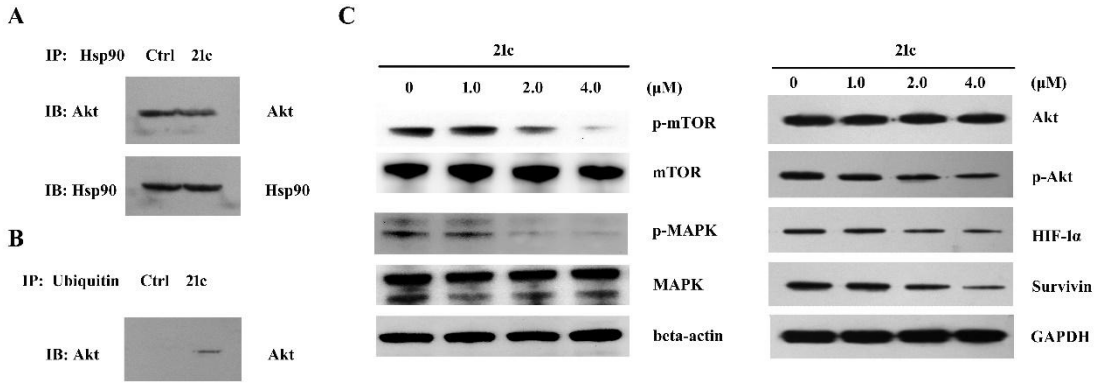

Figure 5. Compound **21c** triggered degradation of multiple Hsp90 client proteins in a concentration dependent manner. (A) Inhibition of Hsp90 and Akt binding in vitro by compound **21c** (4 μM); (B) Induced degradation of Akt protein by compound **21c** (4 μM); (C) Western-blot analysis of the expression levels of several client proteins of Hsp90 after incubation with **21c** in MCF-7 cells.

*2.5.Compound **21c** inhibited cell growth by inducing S and G2-phase cell cycle arrest.*

To determine whether inhibition of cell proliferation was associated with cell cycle arrest, MCF-7 cells were treated with vehicle or various concentrations of **21c** and the relative DNA content of cells were then analyzed by flow cytometry. The results showed that **21c**-treated MCF-7 cells were arrested at the S and G2 phase. As shown in Figure 6, MCF-7 cells treated with 4 μM **21c** for 48 h had 29.6% cells in G2 phase, as compared with 16.6% in the control. Conversely, the amount of cells at the G1 phase significantly decreased from 60.6% (control) to 40.7% (treated with 4 μM **21c**).

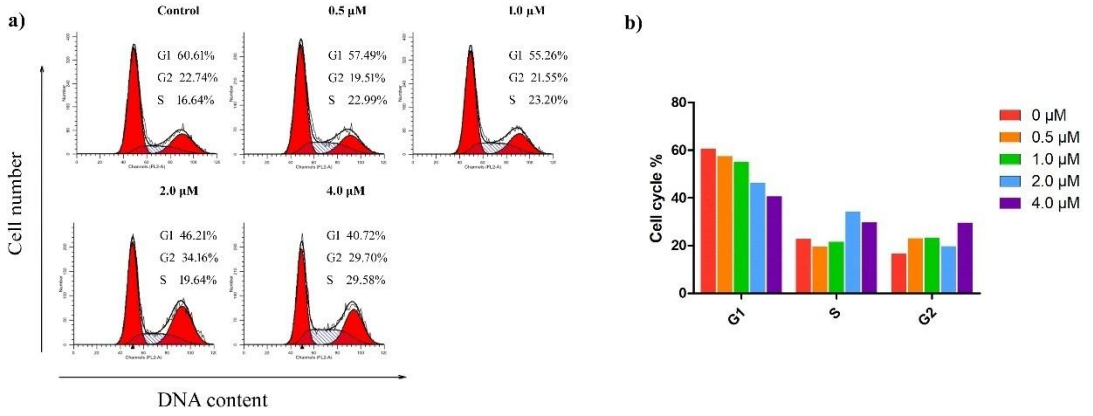

Figure 6. Effects of compound **21c** on cell cycle distribution of MCF-7 cells. Cells treated with DMSO or indicated concentrations of **21c** for 36 h were analyzed for DNA content by flow cytometry.

*2.6. Induction of apoptosis by compound **21c***

In addition to cell cycle arrest, the overall cell growth inhibition induced by **21c** could be caused by increase of apoptosis. Two separate assays were used to investigate the induction of apoptosis in MCF-7 cells by **21c**. First, induction of apoptosis as a results of treatment of **21c** was assessed by Hoechst 33258 staining. MCF-7 cells treated with vehicle or various concentrations of **21c** for 36 h were stained with Hoechst 33258 and the cell morphology was visualized by fluorescent microscopy. Characteristic features of apoptosis such as rounding of cells and nuclei, condensation and

peripherization of chromosome were clearly observed in MCF-7 cells after treatment with **21c** (Figure 7).

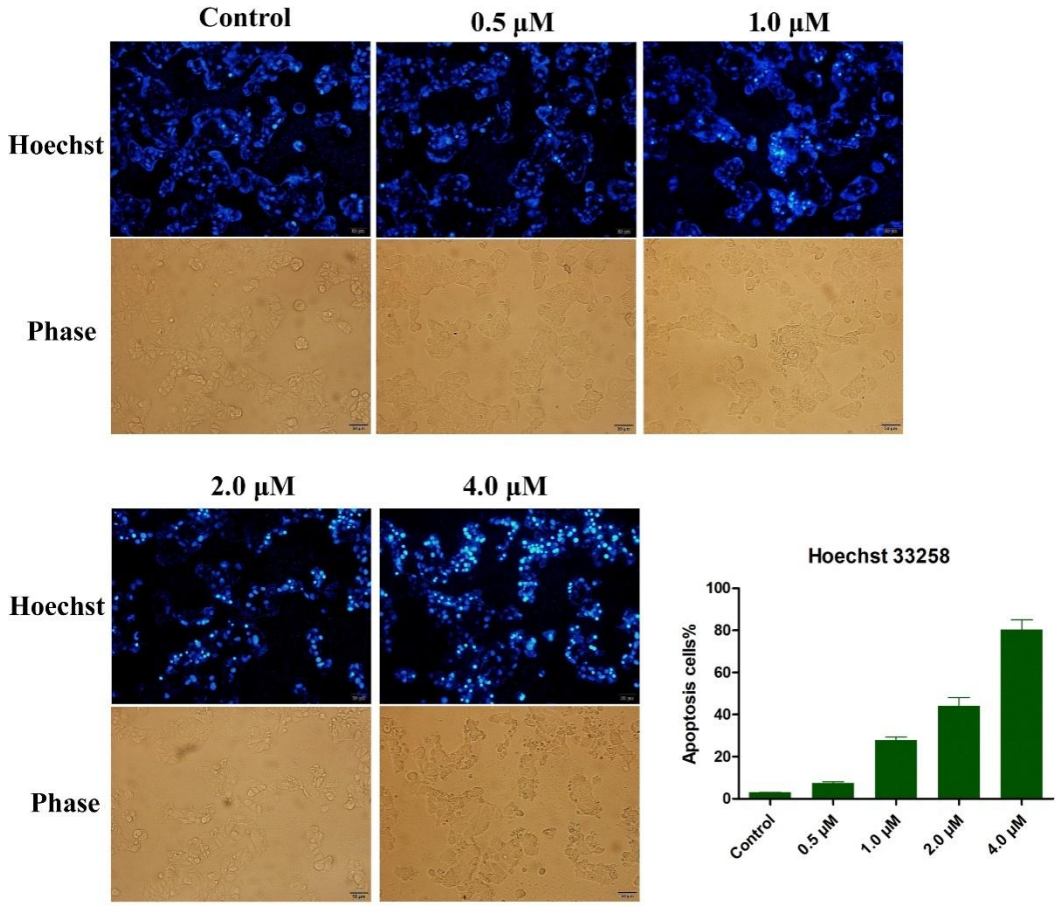

Figure 7. Hoechst 33258 staining of cells treated with **21c**. Cell morphological alterations and nuclear changes associated with MCF-7 cells after incubation with **21c** were assessed by staining with Hoechst 33258 and visualized by fluorescence microscopy, bars denote 50 μM.

To further confirm whether **21c** could induce apoptosis in MCF-7 cells, vehicle- or **21c**-incubated MCF-7 cells were stained with Annexin V and PI. As shown in Figure 8A, incubation with **21c** induced a concentration-dependent (0.5, 1.0, 2.0 and 4.0 μM) increase (from 13.6% to 71.8%) in both the early and late stage apoptosis of MCF-7 cells.Besides, the expression of apoptotic proteins were detected to determine whether caspase-mediated apoptotic pathway was involved in **21c**-treated cancer cells. Consistent with the results obtained from deguelin in previous reports, a marked

decrease in the level of Bcl-xL and increase in the level of cleaved caspase 3 were detected in the cells treated with **21c**[21].

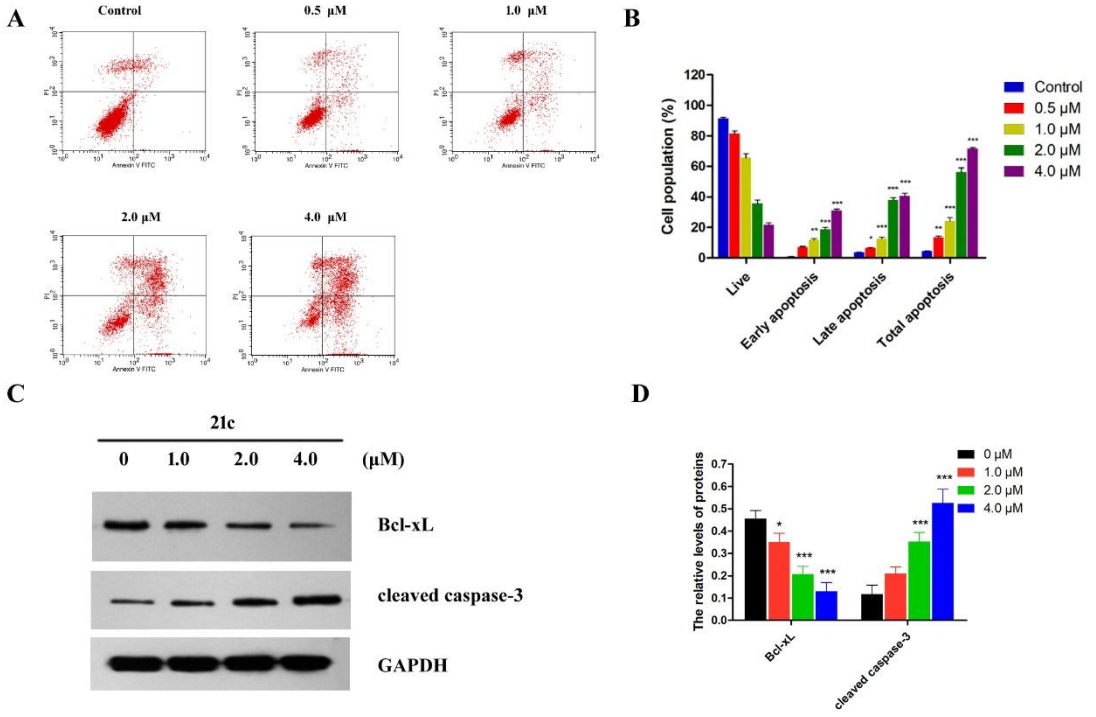

Figure 8. Effect of compound **21c** on apoptosis in MCF-7 cells. (A) Cells were treated with DMSO or various concentrations of **21c** for 36 h; (B) Histograms display the percentage of cell distribution. Data were represented as mean±SD of three independent experiments. **p*<0.05, ***p*<0.01, and ****p*<0.001 *vs* control group; (C) The expression of Bcl-xL and cleaved caspase-3 were analyzed by Western-blot analysis; (D) Histograms display the density ratios of Bcl-xL and cleaved caspase 3 to GAPDH. Data was represented as mean±SD of three independent experiments. **p*<0.05, ****P*<0.001, control compared with **21c** treated cells.

*2.7. Inhibitory effects of **21c** on migration and invasion of MCF-7 cells.*

Tumor invasion through extracellular matrix is an essential step in the tumor metastasis[22]. PI3K-Akt signaling has been shown to regulate cancer cell growth and invasion via increased motility and MMPs production[23]. In addition, deguelin has been reported to inhibit the invasion of cancer cells, thus, in the present study, effects of compound **21c** on the migration and invasion of MCF-7 cells were examined[24].

As shown in Figure 9A, the wound healing significantly decreased (indicative of decreased cell migration) in **21c**-treated MCF-7 cells as compared to control cells, indicating that the migration of cells was significantly inhibited by **21c**. Besides, the mean percentage value of the invaded cells through Matrigel-coated filters without test compound was 172.1±8.3 after 24 h incubation, compound **21c** inhibited invasion of MCF-7 cells in a concentration dependent manner (Figure 9D). Although only a weak antiproliferative effect of **21c** was observed at a concentration of 1 μM (Table 1), it showed much stronger inhibition on the invasion of MCF-7 cells, and the invaded cells were significantly decreased to 63.2±3.4 by 1 μM of **21c** after 24 h incubation (Figure 9D).

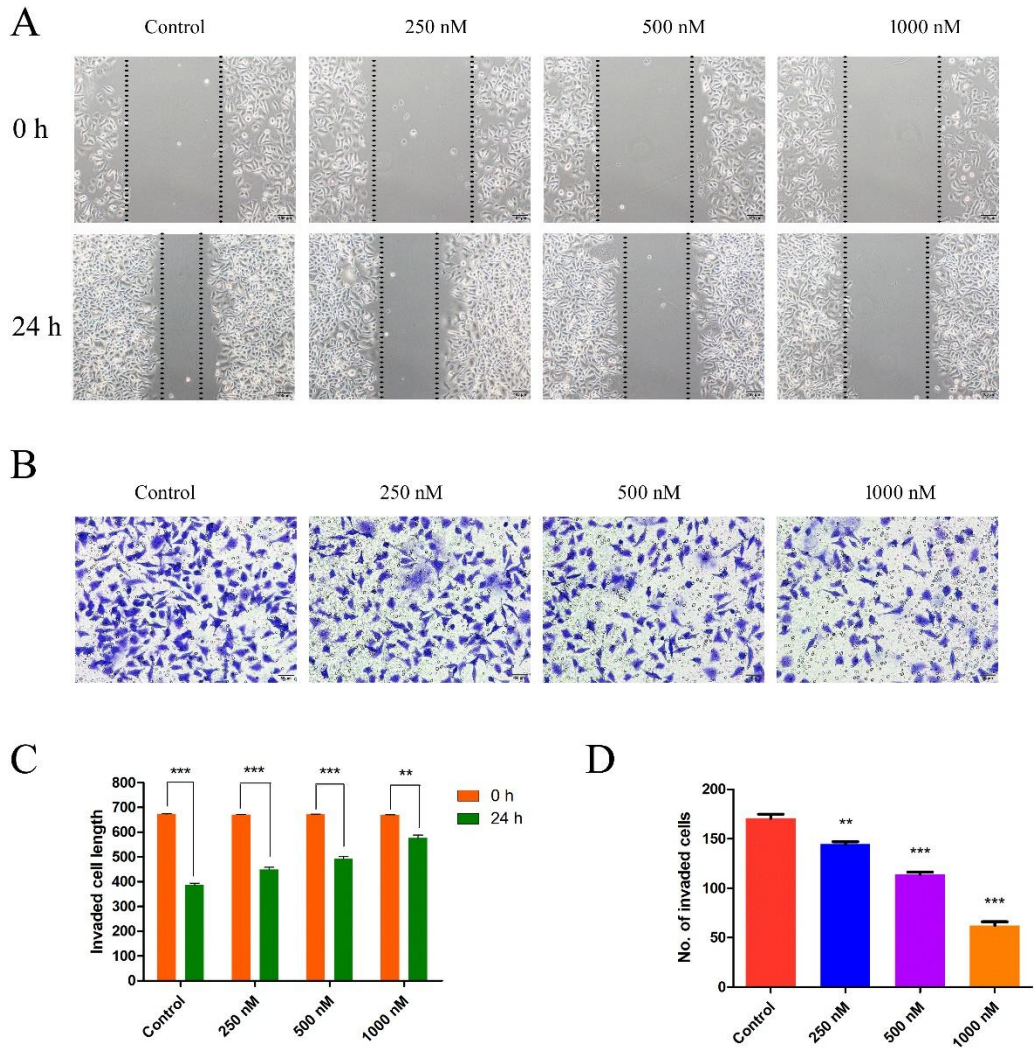

Figure 9. Compound **21c** decreased the migration and invasion of breast cancer cells. (A) Wound healing assay of MCF-7 cells treated with various concentrations of **21c**;

(B) Represent photomicrographs showing the invasive capability of MCF-7 cells was impaired by **21c** in a dose-dependent manner; (C) The wounding area was quantified; (D) The number of migrating cells was determined by counting the stained cells and histogram. ***P<0.001, **P<0.01 compared with control group.

3. Conclusion

In summary, twenty four structurally simpler derivatives of natural product deguelin were obtained and identified as novel Hsp90 inhibitors by the optimization of chemical structure-truncating strategy. Some of the truncated deguelin derivatives displayed same or enhanced anti-proliferative efficacy on a panel of human cancer cell lines, indicating that simplification of B- and C-rings of deguelin retained its anticancer efficacy. The most potent compound **21c**, was 3-fold more potent than parent molecule deguelin against MCF-7 cancer cells. Docking studies explained the high binding affinity of **21c** to Hsp90 due to the relieved conformational restriction by truncating B- and C- rings of deguelin. Compound **21c** was identified to have high Hsp90 binding potency (60 nM) and caused degradation of client proteins through ubiquitin proteasome system. In addition, the molecular mechanism study of **21c** on the suppression of human breast cancer MCF-7 cell growth revealed that compound **21c** caused cancer cells arrest at G2/M phase of the cell cycle, and it significantly increased cell apoptosis, which was illustrated by chromatin condensation, externalization of phosphatidylserine and a marked decrease in the level of Bcl-xL and increase in the level of cleaved caspase 3. In additional, compound **21c** showed much potent inhibition on the migration and invasion of MCF-7 cells. Collectively, our results demonstrated that the newly developed truncated deguelin derivative **21c** possessed significant anticancer efficacy, and has the potential to be further development of Hsp90 inhibitors as anti-tumor agent.

4. Experimental section

4.1. General information

All commercially available reagents were used without further purification.

Anhydrous solvents were dried through routine protocols. Flash column chromatography was carried out on 200-300 mesh silica gel (Qingdao Haiyang Chemical, China). Reactions were monitored by thin-layer chromatography (TLC) on 0.25 mm silicagel plates (GF254) and visualized under UV light. ^{1}H NMR and ^{13}C NMR spectra were recorded with a Bruker AV-300 spectrometer (Bruker Company, Germany) in the indicated solvents ($CDCl_3$ or DMSO-d_6, TMS as internal standard): the values of the chemical shifts are expressed in δ values (ppm) and the coupling constants (J) in Hz. Low-and high-resolution mass spectrums (LRMS and HRMS) were measured on Finnigan MAT 95 spectrometer (Finnigan, Germany).

4.2. Synthesis of target compounds

4.2.1. 1-(2,4-Dihydroxyphenyl)-2-(3,4-dimethoxyphenyl)ethan-1-one (**7b**)

3,4-Dimethoxyphenylacetic acid (1.0 g, 5.1 mmol, 1.0 equiv.) and resorcinol (561 mg, 5.1 mmol, 1.0 equiv.) were added into 15 mL boron trifluoride ethyl etherate. The mixture was stirred at 90 ℃ for 1.5 h under the protection of nitrogen. 30 mL cold water containing 3.0 g sodium acetate was added into the reaction solution to precipitate the product. The mixture was filtered and the solid was purified by ethyl acetate to obtained **7b** as a yellow solid (1.17 g, 80%). ^{1}H NMR (300 MHz, DMSO-d_6) δ 12.38 (s, 1H), 10.01 (s, 1H), 8.03 (d, J = 8.8 Hz, 1H), 6.91 (d, J = 2.0 Hz, 1H), 6.89 (d, J = 8.2 Hz, 1H), 6.79 (dd, J = 8.2, 2.0 Hz, 1H), 6.75 (d, J = 2.4 Hz, 1H), 6.71 (dd, J = 8.9, 2.4 Hz, 1H), 4.25 (s, 2H), 3.72 (s, 3H), 3.72 (s, 3H); ESI-MS *m/z* 311.1 $[M+Na]^+$.

4.2.2. 2-(3,4-Dimethoxyphenyl)-1-(2-hydroxy-4-((2-methylbut-3-yn-2-yl)oxy)phenyl) ethan-1-one (**8b**)

Compound **7b** (1.17 g, 4.06 mmol, 1.0 equiv.), 3-chloro-3-methyl-1-butyne (537 μL, 4.87 mmol, 1.2 equiv.), copper iodide (77 mg, 0.4 mmol, 0.1 equiv.), potassium iodide (67 mg, 0.4 mmol, 0.1 equiv.) and potassium carbonate (673 mg, 4.87 mmol, 1.2 equiv.) were added into 20 mL acetonitrile. The mixture was stirred at room temperature for 12 h. The solvent was removed at reduced pressure, and the residue

was treated with 10 mL water and extracted with ethyl acetate (3 × 30 mL). The combined organic phases were dried (Na_2SO_4), and the solvent was removed at reduced pressure. The crude residue was purified by column chromatography with petroleum/ethyl acetate (10:1) to give **8b** as a white solid (0.72 g, 50%). ^{1}H NMR (300 MHz, DMSO-d_6) δ 12.38 (s, 1H), 8.03 (d, J = 8.8 Hz, 1H), 6.91 (d, J = 2.0 Hz, 1H), 6.89 (d, J = 8.2 Hz, 1H), 6.79 (dd, J = 8.2, 2.0 Hz, 1H), 6.75 (d, J = 2.4 Hz, 1H), 6.71 (dd, J = 8.8, 2.4 Hz, 1H), 4.25 (s, 2H), 3.83 (s, 1H), 3.72 (s, 3H), 3.72 (s, 3H), 1.66 (s, 6H); ESI-MS *m/z* 355.2 $[M+H]^+$.

4.2.3.

2-(3,4-Dimethoxyphenyl)-1-(5-hydroxy-2,2-dimethyl-2H-chromen-6-yl)ethan-1-one (**9b)**

Compound **8b** (0.72 g) was dissolved in 5 mL *N*,*N*-dimethylaniline, and the mixture was refluxed at 130 ℃ for 24 h. After the reaction was completed, 10 mL concentrated HCl was added and extracted with ethyl acetate (3 × 30 mL). The combined organic phases were dried (Na_2SO_4), and the solvent was removed at reduced pressure. The crude residue was purified by column chromatography with petroleum/ethylacetate (10:1) to give **9b** as a white solid (0.68 g, 95%). ^{1}H NMR (300 MHz, $CDCl_3$) δ 12.92 (s, 1H), 7.61 (d, J = 8.8 Hz, 1H), 6.76 (m, 3H), 6.66 (d, J = 10.1 Hz, 1H), 6.30 (d, J = 8.8 Hz, 1H), 5.53 (d, J = 10.1 Hz, 1H), 4.10 (s, 2H), 3.82 (s, 6H), 1.41 (s, 6H); ^{13}C NMR (75 MHz, $CDCl_3$) δ 201.8, 159.6, 159.3, 148.5, 147.6, 130.9, 127.7, 126.3, 121.0, 115.2, 112.5, 111.8, 110.8, 108.9, 107.9, 77.3, 55.4, 43.8, 27.9; HRESI-MS *m/z* calcd for $C_{21}H_{22}O_5$ 355.1540 $[M+H]^+$, found 355.1557.

4.2.4.

1-(5-Hydroxy-2,2-dimethyl-2H-chromen-6-yl)-2-(4-methoxyphenyl)ethan-1-one (**9c**)

Compound **9c** was prepared as the same procedures of **9b** with the commercially available 3,4-dimethoxyphenylacetic acid as the starting material. ^{1}H NMR (300 MHz, $CDCl_3$) δ 12.89 (s, 1H), 7.57 (d, J = 8.9 Hz, 1H), 7.14-7.06 (d, J = 8.1 Hz, 2H), 6.84-6.76 (d, J = 8.1 Hz, 2H), 6.63 (d, J = 10.1 Hz, 1H), 6.26 (d, J = 8.9 Hz, 1H), 5.50

(d, J = 10.1 Hz, 1H), 4.06 (s, 2H), 3.72 (s, 3H), 1.37 (s, 6H); ^{13}C NMR (75 MHz, $CDCl_3$) δ 202.0, 159.6, 159.2, 158.1, 130.9, 129.9, 127.7, 125.9, 115.2, 113.7, 112.5, 108.9, 107.9, 77.3, 54.8, 43.4, 27.85; HRESI-MS *m/z* calcd for $C_{20}H_{20}O_4$, $[M+H]^+$ 325.1434, found 325.1488.

4.2.5.

2-(3,4-Dichlorophenyl)-1-(5-hydroxy-2,2-dimethyl-2H-chromen-6-yl)ethan-1-one (**9d**)

Compound **9d** was prepared as the same procedures of **9b** with the commercially available 3,4-dichlorophenylacetic acid as the starting material. ^{1}H NMR (300 MHz, $CDCl_3$) δ 12.77 (s, 1H), 7.58 (d, J = 8.9 Hz, 1H), 7.42 (d, J = 8.2 Hz, 1H), 7.37 (d, J = 2.1 Hz, 1H), 7.11 (dd, J = 8.2, 2.1 Hz, 1H), 6.71 (d, J = 10.1 Hz, 1H), 6.37 (d, J = 8.9 Hz, 1H), 5.60 (d, J = 10.1 Hz, 1H), 4.17 (s, 2H), 1.47 (s, 6H); ^{13}C NMR (75 MHz, $CDCl_3$) δ 200.1, 159.6, 134.0, 132.2, 130.9, 130.5, 130.1, 128.4, 127.9, 115.1, 112.3, 109.0, 108.3, 77.5, 43.0, 27.9; HRESI-MS *m/z* calcd for $C_{19}H_{16}Cl_2O_3$ 363.0549 $[M+H]^+$, found 363.0590.

4.2.6.

1-(5-Hydroxy-2,2-dimethyl-2H-chromen-6-yl)-2-(3,4,5-trimethoxyphenyl)ethan-1-one (**9e**)

Compound **9e** was prepared as the same procedures of **9b** with the commercially available 3,4,5-trimethoxyphenylacetic acid as the starting material. ^{1}H NMR (300 MHz, $CDCl_3$) δ 12.92 (s, 1H), 7.62 (d, J = 8.8 Hz, 1H), 6.68 (d, J = 10.2 Hz, 1H), 6.45 (s, 2H), 6.32 (d, J = 8.8 Hz, 1H), 5.59 (d, J = 10.2 Hz, 1H), 4.11 (s, 2H), 3.82 (s, 9H), 1.43 (s, 6H); ^{13}C NMR (75 MHz, $CDCl_3$) δ 201.5, 159.6, 159.4, 152.8, 130.8, 129.5, 129.1, 127.8, 115.1, 112.5, 108.8, 108.0, 106.2, 105.9, 77.4, 60.3, 55.6, 44.4, 27.8; HRESI-MS *m/z* calcd for $C_{22}H_{24}O_6$ 385.1646 $[M+H]^+$, found 385.1679.

4.2.7.

3-(3,4-Dimethoxyphenyl)-1-(5-hydroxy-2,2-dimethyl-2H-chromen-6-yl)propan-1-one

(**9f**)

Compound **9f** was prepared as the same procedures of **9b** with the commercially available 3,4-dimethoxyhydrocinnamic acid as the starting material. ^{1}H NMR (300 MHz, $CDCl_3$) δ 13.06 (s, 1H), 7.52 (d, J = 8.9 Hz, 1H), 6.78 (m, 3H), 6.72 (d, J = 10.1 Hz, 1H), 6.31 (d, J = 8.8 Hz, 1H), 5.58 (d, J = 10.1 Hz, 1H), 3.87 (d, J = 3.8 Hz, 6H), 3.20 (t, J = 7.5 Hz, 2H), 2.99 (t, J = 7.5 Hz, 2H), 1.45 (s, 6H); ^{13}C NMR (75 MHz, $CDCl_3$) δ 203.3, 159.2, 159.1, 148.4, 147.0, 133.0, 130.3, 127.7, 119.6, 115.3, 112.9, 111.2, 110.8, 108.8, 107.8, 77.2, 55.4, 55.3, 39.3, 29.6, 27.8; HRESI-MS *m/z* calcd for $C_{22}H_{24}O_5$ 369.1722 $[M+H]^+$, found 369.1739.

4.2.8.

2-(3,4-Dimethoxyphenyl)-1-(5-methoxy-2,2-dimethyl-2H-chromen-6-yl)ethan-1-one (**11**)

Compound **9b** (500 mg, 1.41 mmol, 1.0 equiv.), methyl iodide (131 μL, 2.12 mmol, 1.5 equiv.), and potassium carbonate (292 mg, 2.12 mmol, 1.5 equiv.) were dissolved in acetone (20 mL).The mixture was refluxed for 12 h. After the reaction was completed, allow it to cool to room temperature. The solvent was removed at reduced pressure, and the residue was treated with 10 mL water and extracted with ethyl acetate (3 × 30 mL). The combined organic phases were dried (Na_2SO_4), and the solvent was removed at reduced pressure. The crude residue was purified by column chromatography with petroleum/ethyl acetate (8:1) to give **11** as a white solid (0.36 g, 70%). ^{1}H NMR (300 MHz, $CDCl_3$) δ 7.41 (d, J = 8.6 Hz, 1H), 6.70 (s, 3H), 6.51 (m, 2H), 5.59 (d, J = 10.0 Hz, 1H), 4.11 (s, 2H), 3.75 (s, 6H), 3.68 (s, 3H), 1.35 (s, 6H); ^{13}C NMR (75 MHz, $CDCl_3$) δ 198.2, 157.3, 155.9, 148.3, 147.3, 130.7, 130.1, 127.1, 124.3, 121.2, 116.0, 114.3, 112.2, 112.2, 110.7, 76.4, 62.8, 55.3, 55.3, 47.7, 27.5; HRESI-MS *m/z* calcd for $C_{22}H_{24}O_5$ 369.1697 $[M+H]^+$, found 369.1712.

4.2.9. 1-(5-Methoxy-2,2-dimethyl-2H-chromen-6-yl)-2-phenylethan-1-one (**10a**)

Compound **10a** was prepared as the same procedures of **11** with the commercially available phenylacetic acid as the starting material. ^{1}H NMR (300 MHz, $CDCl_3$) δ

7.56 (d, *J* = 8.6 Hz, 1H), 7.28 (m, 5H), 6.63 (d, *J* = 10 Hz, 1H), 6.60 (d, *J* = 8.7 Hz, 1H), 5.70 (d, *J* = 10.0 Hz, 1H), 4.29 (s, 2H), 3.78 (s, 3H), 1.47 (s, 6H); ^{13}C NMR (75 MHz, $CDCl_3$) δ 201.7, 156.7, 155.4, 140.9, 130.4, 130.0, 128.1, 127.5, 126.2, 124.9, 116.1, 114.4, 111.9, 76.3, 62.8, 50.0, 27.6, 27.5; HRESI-MS *m/z* calcd for $C_{20}H_{20}O_3$ 309.1485 $[M+H]^+$, found 309.1505.

4.2.10. 1-(5-Methoxy-2,2-dimethyl-2H-chromen-6-yl)-2-phenylpropan-1-one (**10b**)

Compound **10b** was prepared as the same procedures of **11** with the commercially available phenylacetic acid and 3 equivalent of methyl iodide as the starting material. ^{1}H NMR (300 MHz, $CDCl_3$) δ 7.38 (d, *J* = 8.6 Hz, 1H), 7.28 (m, 4H), 7.20 (d, *J* = 8.7 Hz, 1H), 6.60 (d, *J* = 10 Hz, 1H), 6.54 (d, *J* = 8.7 Hz, 1H), 5.66 (d, *J* = 10.0 Hz, 1H), 4.73 (d, *J* = 6.9 Hz, 1H), 3.68 (s, 3H), 1.54 (d, *J* = 6.9 Hz, 3H), 1.43 (s, 6H); ^{13}C NMR (75 MHz, $CDCl_3$) δ 201.7, 156.7, 155.4, 140.9, 130.4, 130.0, 128.1, 127.5, 126.2, 124.9, 116.1, 114.4, 111.9, 76.3, 62.8, 50.0, 27.6, 27.5, 18.8; HRESI-MS *m/z* calcd for $C_{21}H_{22}O_3$ 323.1642 $[M+H]^+$, found 323.1678.

4.2.11.

1-(5-Methoxy-2,2-dimethyl-2H-chromen-6-yl)-2-(4-methoxyphenyl)ethan-1-one (**10c**)

Compound **10c** was prepared as the same procedures of **11** with the commercially available 3,4-dimethoxyphenylacetic acid as the starting material. ^{1}H NMR (300 MHz, $CDCl_3$) δ 7.47 (d, *J* = 8.6 Hz, 1H), 7.13 (d, *J* = 8.7 Hz, 2H), 6.81 (d, *J* = 8.7 Hz, 2H), 6.56 (m, 2H), 5.65 (d, *J* = 10.0 Hz, 1H), 4.16 (s, 2H), 3.74 (s, 3H), 3.73 (s, 3H), 1.41 (s, 6H); ^{13}C NMR (75 MHz, $CDCl_3$) δ 202.0, 157.8, 156.6, 155.3, 132.9, 130.4, 130.0, 128.5, 124.9, 116.1, 114.3, 113.5, 111.9, 76.2, 62.9, 54.7, 49.1, 27.5; HRESI-MS *m/z* calcd for $C_{21}H_{22}O_4$ 339.1591 $[M+H]^+$, found 339.1612.

4.2.12.

1-(5-Methoxy-2,2-dimethyl-2H-chromen-6-yl)-2-(4-methoxyphenyl)propan-1-one (**10d**)

Compound **10d** was prepared as the same procedures of **11** with the commercially available 4-methoxyphenylacetic acid as the starting material. ^{1}H NMR (300 MHz, $CDCl_3$) δ 7.28 (d, J = 8.6 Hz, 1H), 7.15 (d, J = 8.2 Hz, 2H), 6.76 (d, J = 8.2 Hz, 2H), 6.50 (d, J = 8.6 Hz, 1H), 6.49 (d, J = 10.0 Hz, 1H), 5.61 (d, J = 10.0 Hz, 1H), 4.60 (d, J = 6.9 Hz, 1H), 3.71 (s, 3H), 3.63 (s, 3H), 1.45 (d, J = 6.9 Hz, 3H), 1.38 (s, 6H); ^{13}C NMR (75 MHz, $CDCl_3$) δ 202.0, 157.8, 156.6, 155.3, 132.9, 130.4, 130.0, 128.5, 124.9, 116.1, 114.3, 113.5, 111.9, 76.2, 62.9, 54.7, 49.1, 27.5, 18.7; HRESI-MS *m/z* calcd for $C_{22}H_{24}O_4$ 353.1747 $[M+H]^+$, found 353.1781.

4.2.13.

2-(3,4-Dimethoxyphenyl)-1-(5-methoxy-2,2-dimethylchroman-6-yl)ethan-1-one (**12**)

To a solution of compound **11** (100 mg) in methanol (10 mL) was added catalytic amount of 10% Pd/C. The mixture was reacted under the atmosphere of hydrogen at room temperature for 12 h. After the reaction was completed, the mixture was filtrated to remove Pd/C and the solvent was removed at reduced pressure to obtained **12** as a white solid (95 mg, 95%). ^{1}H NMR (300 MHz, $CDCl_3$) δ 7.47 (d, J = 8.7 Hz, 1H), 6.77 (s, 3H), 6.56 (d, J = 8.7 Hz, 1H), 4.17 (s, 2H), 3.81 (s, 6H), 3.73 (s, 3H), 2.74 (t, J = 6.6 Hz, 2H), 1.77 (t, J = 6.6 Hz, 2H), 1.31 (s, 6H); ^{13}C NMR (75 MHz, $CDCl_3$) δ 198.4, 158.7, 158.4, 148.6, 147.2, 128.9, 127.2, 123.1, 121.2, 114.7, 112.8, 112.2, 110.7, 74.9, 61.3, 55.3 (two carbons), 47.5, 31.5, 26.2, 16.8; HRESI-MS *m/z* calcd for $C_{22}H_{26}O_5$ 371.1853 $[M+H]^+$, found 371.1889.

4.2.14.

2-(3,4-Dimethoxyphenyl)-1-(5-methoxy-2,2-dimethyl-2H-chromen-6-yl)ethan-1-ol (**13**)

To a solution of compound **11** (1.0 g, 2.71 mmol, 1.0 equiv.) in methanol (20 mL) was added sodium borohydride (205 mg, 5.43 mmol, 2.0 equiv.) at 0 ^{o}C. The reaction mixture was stirred at this temperature for 1 h. After the reaction was completed, the reaction was quenched with saturated ammonium chloride solution. The reaction mixture was treated with 10 mL water and extracted with ethyl acetate (3 × 30 mL).

The combined organic phases were dried (Na_2SO_4), and the solvent was removed at reduced pressure. The crude residue was purified by column chromatography with petroleum/ethyl acetate (6:1) to give **13** as a white solid (0.95 g, 95%).^{1}H NMR (300 MHz, $CDCl_3$) δ 7.13 (d, J = 8.4 Hz, 1H), 6.72 (s, 2H), 6.61 (s, 1H), 6.56 (d, J = 8.4 Hz, 1H), 6.48 (d, J = 9.9 Hz, 1H), 5.59 (d, J = 9.9 Hz, 1H), 5.06-4.97 (m, 1H), 3.78 (s, 3H), 3.75 (s, 3H), 3.59 (s, 3H), 2.99-2.80 (m, 2H), 2.24 (s, 1H), 1.37 (s, 6H); ^{13}C NMR (75 MHz, $CDCl_3$) δ 152.9, 148.2, 147.1, 130.6, 129.9, 128.0, 126.4, 121.0, 116.6, 113.9, 112.3, 112.2, 110.6, 75.2, 69.1, 62.1, 55.4, 55.2, 43.9, 27.2, 27.1; HRESI-MS *m/z* calcd for $C_{22}H_{26}O_5$ 371.1853 $[M+H]^+$, found 371.1877.

4.2.15. (E)-6-(3,4-Dimethoxystyryl)-5-methoxy-2,2-dimethyl-2H-chromene (**14**)

To a solution of acetic acid was added compound **13** (500 mg), and the mixture was heated to 60 ^{o}C. After the reaction was completed, saturated sodium bicarbonate solution was added to quench to the reaction. The reaction mixture was treated with 10 mL water and extracted with ethyl acetate (3 × 30 mL). The combined organic phases were dried (Na_2SO_4), and the solvent was removed at reduced pressure. The crude residue was purified by column chromatography with petroleum/ethyl acetate (6:1) to give **14** as a white solid (0.45 g, 90%). ^{1}H NMR (300 MHz, $CDCl_3$) δ 7.39 (d, J = 8.6 Hz, 1H), 7.18 (d, J = 16.4 Hz, 1H), 7.07 (m, 2H), 6.96 (d, J = 16.4 Hz, 1H), 6.87 (d, J = 8.6 Hz, 1H), 6.64 (m, 2H), 5.67 (d, J = 10.0 Hz, 1H), 3.96 (s, 3H), 3.91 (s, 3H), 3.79 (s, 3H), 1.46 (s, 6H); ^{13}C NMR (75 MHz, $CDCl_3$) δ 153.3, 153.0, 148.6, 148.1, 130.7, 130.0, 126.9, 125.7, 122.8, 120.7, 119.0, 116.5, 114.3, 112.4, 110.8, 108.3, 75.6, 61.9, 55.5, 55.4, 27.4; HRESI-MS *m/z* calcd for $C_{22}H_{24}O_4$, 353.1747 $[M+H]^+$, found 353.1759.

4.2.16. 6-(2-(3,4-Dimethoxyphenyl)acetyl)-2,2-dimethyl-2H-chromen-5-yl acetate (**15**)

To a solution of compound **9b** (100 mg, 0.28 mmol, 1.0 equiv.) in dichloromethane (15 mL) was added triethylamine (78 μL, 0.56 mmol, 2.0 equiv.) and acetic anhydride (80 μL, 0.84 mmol, 3.0 equiv.). The mixture was stirred at room temperature for 10 h.

After the reaction was completed, saturated sodium bicarbonate solution was added to quench the reaction. The reaction mixture was treated with 10 mL water and extracted with ethyl acetate (3 × 30 mL). The combined organic phases were dried (Na_2SO_4), and the solvent was removed at reduced pressure. The crude residue was purified by column chromatography with petroleum/ethyl acetate (6:1) to give **15** as a white solid (100 mg, 90%). ^{1}H NMR (300 MHz, $CDCl_3$) δ 7.71 (d, J = 8.6 Hz, 1H), 6.83 (d, J = 8.0 Hz, 1H), 6.75 (m, 2H), 6.70 (d, J = 8.6 Hz, 1H), 6.39 (d, J = 10.1 Hz, 1H), 5.71 (d, J = 10.1 Hz, 1H), 4.10 (s, 2H), 3.86 (s, 6H), 2.37 (s, 3H), 1.46 (s, 6H); ^{13}C NMR (75 MHz, $CDCl_3$) δ 195.4, 168.9,157.1, 148.4, 147.4, 145.6, 131.3, 130.8, 126.7, 121.0, 115.1, 114.9, 113.1, 112.0, 110.7, 77.0, 55.3, 46.4, 27.8, 20.5; HRESI-MS *m/z* calcd for $C_{23}H_{24}O_6$ 397.1646 $[M+H]^+$, found 397.1659.

4.2.17.

1-(5-(Benzyloxy)-2,2-dimethyl-2H-chromen-6-yl)-2-(3,4-dimethoxyphenyl)-3-phenyl propan-1-one (**16**)

To a solution of compound **9b** (100 mg, 0.282 mmol, 1.0 equiv.) in acetonitrile was added potassium carbonate (58.4 mg, 0.423 mmol, 1.5 equiv.), and benzyl bromide (67 μL, 0.56 mmol, 2.0 equiv.). The mixture was refluxed for 6 h. After the reaction was completed, the reaction mixture was treated with 10 mL water and extracted with ethyl acetate (3 × 30 mL). The combined organic phases were dried (Na_2SO_4), and the solvent was removed at reduced pressure. The crude residue was purified by column chromatography with petroleum/ethyl acetate (6:1) to give **16** as a white solid (120 mg, 80%).^{1}H NMR (300 MHz, $CDCl_3$) δ 7.40-7.35 (m, 6H), 7.15 (m, 3H), 7.07 (m, 2H), 6.73 (m, 3H), 6.52 (m, 2H), 5.56 (d, J = 10.1 Hz, 1H), 4.84 (t, J = 7.4 Hz, 1H), 4.61 (q, J = 11.4 Hz, 2H), 3.81 (s, 3H), 3.72 (s, 3H), 3.51 (m, 1H), 3.01 (m, 1H), 1.39 (s, 3H), 1.38 (s, 3H); ^{13}C NMR (75 MHz, $CDCl_3$) δ 200.4, 156.6, 153.7, 148.3, 147.4, 139.6, 136.2, 131.0, 130.4, 130.0, 128.8, 128.0, 127.7, 127.3, 125.5, 125.4, 120.3, 116.2, 114.8, 112.0, 110.8, 110.6, 77.2, 76.2, 57.8, 55.2, 39.3, 27.6, 27.48; HRESI-MS *m/z* calcd for $C_{35}H_{34}O_5$ $[M+H]^+$ 535.2479, found 535.2511.

4.2.18. 1-(2-Hydroxy-4-((2-methylbut-3-yn-2-yl)oxy)phenyl)ethan-1-one (**18**)

2,4-Dihydroxyacetophenone (1.0 g, 6.57 mmol, 1.0 equiv.), copper iodide (125 mg, 0.65 mmol, 0.1 equiv.), potassium iodide (109 mg, 0.65 mmol, 0.1 equiv), 3-chloro-3-methyl-1-butyne (652.3 μL, 5.92 mmol, 0.9 equiv.), and potassium carbonate (1.09 g, 7.89 mmol, 1.2 equiv) was dissolved in 20 mL acetonitrile. The mixture was stirred at room temperature for 12 h. After the reaction was completed, the solvent was removed at reduced pressure, and the residue was treated with 10 mL water and extracted with ethyl acetate (3 × 30 mL). The combined organic phases were dried (Na_2SO_4), and the solvent was removed at reduced pressure. The crude residue was purified by column chromatography with petroleum/ethyl acetate (20:1) to give **18** as a white solid (0.86 g, 60%). ^{1}H NMR (300 MHz, $CDCl_3$) δ 13.22 (s, 1H), 7.48 (d, J = 8.9 Hz, 1H), 6.6 (d, J = 8.9 Hz, 1H), 6.53 (s, 1H), 3.61 (s, 1H), 2.63 (s, 3H), 1.41 (s, 6H); ESI-MS *m/z* 219.1 $[M+H]^+$.

4.2.19. 1-(5-Hydroxy-2,2-dimethyl-2H-chromen-6-yl)ethan-1-one (**19**)

To a solution of *N*,*N*-dimethylaniline (5 mL) was added compound **18** (0.858 g), and the mixture was heated to 130 °C and stirred for 12 h. After the reaction was completed, the solvent was removed at reduced pressure, and the residue was treated with 10 mL 10% HCl and extracted with ethyl acetate (3 × 30 mL). The combined organic phases were dried (Na_2SO_4), and the solvent was removed at reduced pressure. The crude residue was purified by column chromatography with petroleum/ethyl acetate (20:1) to give **19** as a white solid (0.81 g, 95%). ^{1}H NMR (300 MHz, $CDCl_3$) δ 13.23 (s, 1H), 7.74 (d, J = 8.8 Hz, 1H), 6.94 (d, J = 10.0 Hz, 1H), 6.56 (d, J = 8.8 Hz, 1H), 5.82 (d, J = 10.0 Hz, 1H), 2.77 (s, 3H), 1.69 (s, 6H); ESI-MS *m/z* 219.1 $[M+H]^+$.

4.2.20. 1-(5-Methoxy-2,2-dimethyl-2H-chromen-6-yl)ethan-1-one (**20**)

Compound **19** (0.81 g, 1.41 mmol, 1.0 equiv.), potassium iodide (61 mg, 0.37 mmol, 0.1 equiv.), and potassium carbonate (615 mg, 4.45 mmol, 1.2 equiv.) were dissolved in 20 mL acetone. The reaction was refluxed for 12 h. After the reaction was completed, the solvent was removed at reduced pressure, and the residue was treated

with 10 mL water and extracted with ethyl acetate (3 × 30 mL). The combined organic phases were dried (Na_2SO_4), and the solvent was removed at reduced pressure. The crude residue was purified by column chromatography with petroleum/ethyl acetate (20:1) to give **20** as a white solid (0.60 g, 70%). ^{1}H NMR (300 MHz, $CDCl_3$) δ 7.58 (d, J = 8.6 Hz, 1H), 6.60 (d, J = 9.8 Hz, 2H), 5.69 (d, J = 10.0 Hz, 1H), 3.80 (s, 3H), 2.60 (s, 3H), 1.45 (s, 6H); ESI-MS *m/z*233.1 $[M+H]^+$.

4.2.21.

2-(3,5-Dimethoxyphenyl)-1-(5-methoxy-2,2-dimethyl-2H-chromen-6-yl)ethan-1-one (**21a**)

To a solution of 3,5-dimethoxybromobenzene (0.2 g, 0.92 mmol, 1.0 equiv.) in THF (20 mL) was added compound **20** (192 mg, 0.82 mmol, 0.9 equiv.), potassium tert-butoxide (155 mg, 1.38 mmol, 1.5 equiv.), tris(dibenzylideneacetone)dipalladium (0.01 equiv.) and bis(2-diphenylphosphinophenyl)ether (0.01 equiv.). The mixture was refluxed for 6 h. After the reaction was completed, the solvent was removed at reduced pressure, and the residue was treated with 10 mL water and extracted with ethyl acetate (3 × 30 mL). The combined organic phases were dried (Na_2SO_4), and the solvent was removed at reduced pressure. The crude residue was purified by column chromatography with petroleum/ethyl acetate (6:1) to give **21a** as a pale yellow solid (0.24 g, 70%). ^{1}H NMR (300 MHz, $CDCl_3$) δ 7.51 (d, J = 8.6 Hz, 1H), 6.60 (m, 2H), 6.42 (d, J = 2.1 Hz, 2H), 6.34 (s, 1H), 5.68 (d, J = 10.0 Hz, 1H), 4.20 (s, 2H), 3.76 (s, 3H), 3.77 (s, 6H), 1.45 (s, 6H); ^{13}C NMR (75 MHz, $CDCl_3$) δ 198.2, 157.3, 155.9, 148.3, 147.3, 130.7, 130.1, 127.1, 124.3, 121.2, 116.0, 114.3, 112.2, 112.2, 110.6, 76.4, 62.8, 55.3, 55.9, 47.7, 27.5; HRESI-MS *m/z* calcd for $C_{22}H_{24}O_5$ 369.1697 $[M+H]^+$, found 369.1741.

4.2.22.

2-(2,5-Dimethoxyphenyl)-1-(5-methoxy-2,2-dimethyl-2H-chromen-6-yl)ethan-1-one (**21b**)

Compound **21b** was prepared as the same procedures of **21a** with the commercially

available 2,5-dimethoxybromobenzene as the starting material. ^{1}H NMR (300 MHz, $CDCl_3$) δ 7.58 (d, J = 8.7 Hz, 1H), 6.79 (m, 3H), 6.62 (dd, J = 8.7, 6.1 Hz, 2H), 5.69 (d, J = 10.0 Hz, 1H), 4.24 (s, 2H), 3.84 (s, 3H), 3.76 (s, 3H), 3.73 (s, 3H), 1.46 (s, 6H); ^{13}C NMR (75 MHz, $CDCl_3$) δ 197.6, 157.0, 155.9, 152.9, 151.2, 130.6, 129.9, 125.0, 124.7, 116.9, 116.2, 114.4, 112.0, 111.9, 110.9, 76.3, 62.7, 55.5, 55.2, 43.2, 27.5; HRESI-MS *m/z* calcd for $C_{22}H_{24}O_5$, 369.1697 $[M+H]^+$, found 369.1731.

4.2.23.

1-(5-Methoxy-2,2-dimethyl-2H-chromen-6-yl)-2-(2,4,5-trimethoxyphenyl)ethan-1-one (**21c**)

Compound **21c** was prepared as the same procedures of **21a** with the commercially available 2,4,5-trimethoxybromobenzene as the starting material. ^{1}H NMR (300 MHz, $CDCl_3$) δ 7.57 (d, J = 8.6 Hz, 1H), 6.74 (s, 1H), 6.68-6.57 (m, 2H), 6.54 (s, 1H), 5.69 (d, J = 10.0 Hz, 1H), 4.20 (s, 2H), 3.89 (s, 3H), 3.84 (s, 3H), 3.82 (s, 3H), 3.75 (s, 3H), 1.46 (s, 6H); ^{13}C NMR (75 MHz, $CDCl_3$) δ 198.1, 157.0, 155.8, 151.1, 148.0, 142.3, 130.5, 130.0, 124.7, 116.2, 115.1, 114.5, 114.4, 112.0, 97.2, 76.2, 62.7, 56.0, 55.9, 55.6, 42.5, 27.5; HRESI-MS *m/z* calcd for $C_{23}H_{26}O_6$, 399.1802 $[M+H]^+$, found 399.1859.

4.2.24.

1-(5-Methoxy-2,2-dimethyl-2H-chromen-6-yl)-2-(3,4,5-trimethoxyphenyl)ethan-1-one (**21d**)

Compound **21d** was prepared as the same procedures of **21a** with the commercially available 3,4,5-trimethoxybromobenzene as the starting material. ^{1}H NMR (300 MHz, $CDCl_3$) δ 7.58 (d, J = 8.7 Hz, 1H), 6.79 (m, 2H), 6.47 (s, 2H), 5.69 (d, J = 10.0 Hz, 1H), 4.24 (s, 2H), 3.82 (s, 6H), 3.76 (s, 3H), 3.73 (s, 3H), 1.46 (s, 6H); ^{13}C NMR (75 MHz, $CDCl_3$) δ 197.8, 157.4, 156.0, 152.6, 136.2, 130.7, 130.2, 130.2, 124.2, 116.0, 114.4, 112.2, 106.1, 76.4, 62.8, 60.3, 55.5, 48.4, 27.5; HRESI-MS *m/z* calcd for $C_{23}H_{26}O_6$, 399.1802 $[M+H]^+$, found399.1843.

4.2.25.

2-(2,3-Dihydrobenzo[b][1,4]dioxin-6-yl)-1-(5-methoxy-2,2-dimethyl-2H-chromen-6-yl)ethan-1-one (**21e**)

Compound **21e** was prepared as the same procedures of **21a** with the commercially available 6-bromo-2,3-dihydrobenzo[b][1,4]dioxine as the starting material. ^{1}H NMR (300 MHz, $CDCl_3$) δ 7.52 (d, J = 8.7 Hz, 1H), 7.02 (m, 1H), 6.94 (d, J = 8.4 Hz, 1H), 6.84-6.68 (m, 2H), 6.61 (m, 1H), 5.69 (d, J = 10.0 Hz, 1H), 4.30 (d, J = 7.4 Hz, 2H), 4.24 (s, 3H), 4.16 (s, 2H), 3.78 (s, 2H), 1.46 (s, 6H); ^{13}C NMR (75 MHz, $CDCl_3$) δ 198.0, 157.3, 156.0, 142.9, 141.8, 130.7, 130.0, 127.7, 122.1, 117.9, 116.7, 116.1, 116.0, 114.4, 112.2, 76.4, 63.8, 62.8, 47.3, 27.6; HRESI-MS *m/z* calcd for $C_{22}H_{22}O_5$ 367.1540 $[M+H]^+$, found 367.1579.

4.2.26.

1-(5-Methoxy-2,2-dimethylchroman-6-yl)-2-(3,4,5-trimethoxyphenyl)ethan-1-one (**22**)

To a solution of compound **21d** (100 mg) in methanol (10 mL) was added catalytic amount of 10% Pd/C. The mixture was reacted under the atmosphere of hydrogen at room temperature for 12 h. After the reaction was completed, the mixture was filtrated to remove Pd/C and the solvent was removed at reduced pressure to obtained **22** as a white solid (95 mg, 95%). ^{1}H NMR (300 MHz, $CDCl_3$) δ 7.47 (d, J = 8.7 Hz, 1H), 6.55 (d, J = 8.7 Hz, 1H), 6.45 (s, 2H), 4.17 (s, 2H), 3.77 (s, 9H), 3.74 (s, 3H), 2.74 (t, J = 6.7 Hz, 2H), 1.76 (t, J = 6.7 Hz, 2H), 1.30 (s, 6H); ^{13}C NMR (75 MHz, $CDCl_3$) δ 197.9, 158.7, 158.5, 152.5, 136.1, 130.4, 128.9, 123.1, 114.7, 112.9, 106.0, 74.5, 61.3, 60.2, 55.5, 48.1, 31.4, 26.2, 16.8; HRESI-MS *m/z* calcd for $C_{23}H_{28}O_6$ 401.1959 $[M+H]^+$, found 401.1981.

4.2.27.

(E)-3-(3,4-Dimethoxyphenyl)-1-(5-hydroxy-2,2-dimethyl-2H-chromen-6-yl)prop-2-en-1-one (**23a**)

To a solution of compound **19** (1.0 g, 4.58 mmol, 1.0 equiv.) in anhydrous THF (10

mL) was added sodium hydride (164 mg, 6.87 mmol, 1.5 equiv.) at 0 ^{o}C. Then 3,4-dimethoxybenzaldehyde (761.4 mg, 4.58 mmol, 1.0 equiv.) in THF (2 mL) was added dropwise. The mixture was slowly warmed up to room temperature and stirred for 6 h. After the reaction was completed, the solvent was removed at reduced pressure, and the residue was treated with 10 mL water and extracted with ethyl acetate (3 × 30 mL). The combined organic phases were dried (Na_2SO_4), and the solvent was removed at reduced pressure. The crude residue was purified by column chromatography with petroleum/ethyl acetate (6:1) to give **23a** as a red solid (1.18 g, 70%). ^{1}H NMR (300 MHz, $CDCl_3$) δ 13.74 (s, 1H), 7.84-7.67 (m, 2H), 7.43 (d, J = 15.4 Hz, 1H), 6.85 (s, 2H), 6.74 (d, J = 10.0 Hz, 1H), 6.38 (d, J = 8.8 Hz, 1H), 5.59 (d, J = 10.0 Hz, 1H), 3.92 (s, 6H), 1.47 (s, 6H); ^{13}C NMR (75 MHz, $CDCl_3$) δ 191.2, 160.4, 159.3, 153.0, 143.9, 140.0, 130.2, 129.8, 127.6, 118.9, 115.3, 113.5, 108.9, 107.8, 105.2, 77.4, 55.7, 27.9; HRESI-MS *m/z* calcd for $C_{22}H_{22}O_5$ 367.1540 $[M+H]^+$, found 367.1567.

4.2.28.

(E)-1-(5-Hydroxy-2,2-dimethyl-2H-chromen-6-yl)-3-(3,4,5-trimethoxyphenyl)prop-2-en-1-one (**23b**)

Compound **23b** was prepared as the same procedures of **23a** with the commercially available 3,4,5-trimethoxybenzaldehyde as the starting material. ^{1}H NMR (300 MHz, $CDCl_3$) δ 13.74 (s, 1H), 7.84-7.67 (m, 2H), 7.43 (d, J = 15.4 Hz, 1H), 6.85 (s, 2H), 6.74 (d, J = 10.0 Hz, 1H), 6.38 (d, J = 8.8 Hz, 1H), 5.59 (d, J = 10.0 Hz, 1H), 3.92 (s, 9H), 1.47 (s, 6H); ^{13}C NMR (75 MHz, $CDCl_3$) δ 191.2, 160.4, 159.3, 153.0, 143.9, 140.0, 130.2, 129.8, 127.6, 118.9, 115.3, 113.5, 108.9, 107.8, 105.2, 77.3, 60.5, 55.7, 27.9; HRESI-MS *m/z* calcd for $C_{23}H_{24}O_6$ 397.1646 $[M+H]^+$, found 397.1678.

4.3. Cell lines and cell culture

Human NSCLC cells H1299, A549 and human breast cancer cells HT-29 were obtained from the American Type Culture Collection (ATCC, USA). Cells were grown in RPMI 1640 medium (Life Technologies, USA). The media for all cell lines

were supplemented with 10% fetal bovine serum (Life Technologies, USA), 100 μg/mL streptomycin (Life Technologies, USA), and 100 U/mL penicillin (Life Technologies, USA) and maintained at 37°C in a humidified atmosphere with 5% CO_2.

4.4. Determination of in vitro anticancer activity

The overall growth of human cancer cell lines was determined using the colorimetric MTT assay. Briefly, the cell lines were incubated at 37 °C in a humidified 5 % CO_2 incubator for 24 h in 96-microwell plates prior to the experiments. H1299, MCF-7, and A549 cells were seeded at a density of 4,000 cells/well. After the removal of medium, 100 μL of fresh medium containing the test compound at different concentrations was added to each well and incubated at 37 °C for 72 h. The percentage of DMSO in the medium was not exceeded 0.25%. The number of living cells after 72 h of culture in the presence (or absence: control) of the various compounds is directly proportional to the intensity of the blue, which is quantitatively measured by spectrophotometry (Biorad, Nazareth, Belgium) at a 570 nm wavelength. The experiment was performed in quadruplicate and repeated three times.

4.5. The fluorescence polarization (FP) competitive binding assay

In vitro inhibitory activity of compounds on Hsp90 was carried out in 384-well plates by fluorescence polarization assay using Hsp90α and Geldanamycin-FITC (Abcam, Cambridge, UK) according to the manufacturer's instructions. The assay buffer contained 20 mM HEPES pH 7.3, 50 mM KCl, 5 mM $MgCl_2$, 20 mM Na_2MoO_4, 0.01% Triton X-100. Before each use, 100 mg/mL BSA and 2 mM DTT were freshly added. In brief, 10 mL of 5 nM FITC-labeled geldanamycin and 10 mL appropriate serials of diluted compounds was added to the plate. The reactions were initiated by adding 20 μL of Hsp90 recombinant enzyme, after 1 h incubation in 4 ^{o}C in the dark, the fluorescence was measured with excitation wavelength at 485 nm and emission wavelength at 535 nm on EnVision Multilabel Reader (Perkin Elmer, Inc.). IC_{50} were calculated using Graphpad Prims 5. (Graphpad Software, Inc).

4.6. Wound healing assay

Cells were seeded on six-well plates with DMEM containing 10% FBS and grown to confluence. The cells were scratched with a sterile 200 μL pipette tip to create artificial wounds. At 0, 24 and 48 h after wounding, phase-contrast images of the wound healing process were photographed digitally using an inverted Olympus IX50 microscope with 10× objective lens. Eight images per treatment were analyzed to determine averaging parameters of positioning of the migrating cells at the wound edges by digitally drawing lines using the Image J software.

4.7. Transwell matrix penetration assay

1×10^4 Cells were plated on the top side of the polycarbonate transwell filter with matrigel coating in the upper chamber of the BioCoat^{TM} Invasion Chambers (BD, Bedford, MA) and incubated at 37 ^{o}C for 24 h, followed by removal of cells inside the upper chamber with cotton swabs. Invaded cells on the membrane bottom-surface were fixed with 1% paraformaldehyde, stained with crystal violet, and counted (Ten random 200× fields per well). Cell counts were expressed as the mean number of cells per field of view. Three independent experiments were performed.

*4.8. Molecular Modelling of **21c** in Hsp90*

The crystallographic coordinates of Hsp90 were downloaded from Protein Data Bank (PDB ID: 5J2X, 1.22 Å). The structure was edited accordingly by the Protein and Ligand Preparation module in Schrodinger and was minimized using the OPLS-2005 force field. The Glide program was used to study the possible mode of interaction of the compounds with Hsp90, The active site was confined in the mass center of co-crystal ligand, and the size of bounding box was defined as 10 Å × 10 Å × 10 Å. Then compound **21c** and deguelin were prepared using the Ligprep module in Schrodinger Suite, and were minimized using the OPLS-2005 force field. The dockings were performed using the Glide standard precision (Glide-SP) mode with the ligands as flexible, the force field was set as OPLS-2005, and all other parameters

were set to default. The poses were visualized with PyMOL Molecular Graphics System version 2.7.

4.9. Immunoprecipitation

Immunoprecipitation of Akt experiment was performed according to the manufacturer's instructions. The cells were harvested and lysed by IP lysis buffer (250 mmol/L HEPES, 50 mmol/L NaCl, 1 mmol/L EDTA, 0.1 mmol/L neocuproine, 1% NP-40, Protease Inhibitor Cocktail). Antibodies specific to Hsp90 or Akt (Santa Cruz) were added to supernatants followed by an incubation. Immune complexes were then precipitated with protein A agarose beads. Bound proteins were eluted by boiling with loading buffer and analyzed by Western blotting with anti-Hsp90 or Akt antibodies.

4.10. Hoechst 33258 staining

Approximately 5×10^4 cells per well were plated in six-well plates, and the cells were then incubated with 0, 0.5, 1.0, 2.0, and 4.0 μM **21c** for 36 h. After incubation, cells were washed with PBS, fixed in 4% paraformaldehyde for 30 min and then stained with 20 μg/ml Hoechst 33258 for 15 min at room temperature in the dark. Cells were then assessed by fluorescence microscopy for morphological changes after **21c** treatment.

4.11. Flow cytometry analysis for cell apoptosis

MCF-7 cells (1×10^5/well) were cultured in complete medium in six-well plates for 24 h and treated in triplicate with different concentrations of **21c** for 36 h. The control cells were treated with vehicle (1‰ DMSO in complete medium). The cells were harvested, washed and stained with propidium iodide (PI), and FITC-Annexin-V in the dark for 15 min using the FITC-AnnexinV Kit (BD Parmingen, San Diego, CA, USA). The percentages of apoptotic cells were determined by flow cytometry on an FC500 cytometer (Beckman Coulter).

4.12. Cell cycle analysis

5×10^4 MCF-7 cells were seeded into six-well plates and incubated overnight. Cells were then treated with various concentrations of **21c** for 48 h. The cells were harvested, washed with cold PBS and then fixed with 70 % ethanol in PBS at -20 °C for 12 h. Subsequently, the cells were resuspended in PBS containing 100 μg/mL RNase and 50 μg/mL PI and incubated at 37 °C for 30 min. Cell cycle distribution of nuclear DNA was determined by flow cytometry on an FC500 cytometer (Beckman Coulter).

4.13. Western blot analysis

MCF-7 cells were incubated with various concentrations of **21c** and collected after 48 h. Cells were centrifuged and washed two times with ice cold phosphate buffered saline. The pellet was then resuspended in lysis buffer. After the cells were lysed on ice for 20 min, lysates were centrifuged at 13,000 g at 4 °C for 15 min. The protein concentration in the supernatant was determined using the BCA protein assay reagents. Equal amounts of protein (20 μg) were resolved using sodium dodecyl sulfate-polyacrylamide gel electrophoresis (SDS-PAGE) (8-12 % acrylamide gels) and transferred to PVDF Hybond-P membrane. Membranes were blocked for 1 h at room temperature. Membranes were then incubated with primary antibodies against Bcl-xL, cleaved caspase-3, mTOR, p-mTOR, MAPK, p-MAKP, Akt, p-AKT, HIF-1α, Survivin, β-actin, and GAPDH with gentle rotation overnight at 4°C. The bound antibodies were detected using horseradish peroxidase (HRP)-conjugated second antibodies and visualized by the enhanced chemiluminescent reagent.

Acknowledgment

This work is supported by the National Natural Science Foundation of China (No. 81673306, 81703348, and 81874289), "Double First-Class" University project CPU2018GY04, CPU2018GY35, China Pharmaceutical University.

Appendix A. Supplementary data

Supplementary data related to this article can be found at

References

[1] J. Wu, T. Liu, Z. Rios, Q. Mei, X. Lin, S. Cao, Heat shock proteins and cancer, Trends Pharmacol. Sci., 38 (2017) 226-256.

[2] F.H. Schopf, M.M. Biebl, J. Buchner, The HSP90 chaperone machinery, Nat. Rev. Mol. Cell Biol., 18 (2017) 345.

[3] G.D. Lianos, G.A. Alexiou, A. Mangano, A. Mangano, S. Rausei, L. Boni, G. Dionigi, D.H. Roukos, The role of heat shock proteins in cancer, Cancer Lett., 360 (2015) 114-118.

[4] L. Chen, J. Li, E. Farah, S. Sarkar, N. Ahmad, S. Gupta, J. Larner, X. Liu, Cotargeting HSP90 and its client proteins for treatment of prostate cancer, Mol. Cancer Ther., (2016).

[5] K.-S. Park, H. Yang, J. Choi, S. Seo, D. Kim, C.H. Lee, H. Jeon, S.-W. Kim, D.H. Lee, The HSP90 inhibitor, NVP-AUY922, attenuates intrinsic PI3K inhibitor resistance in KRAS-mutant non-small cell lung cancer, Cancer Lett., 406 (2017) 47-53.

[6] T. Kimura, M. Uesugi, K. Takase, N. Miyamoto, K. Sawada, Hsp90 inhibitor geldanamycin attenuates the cytotoxicity of sunitinib in cardiomyocytes via inhibition of the autophagy pathway, Toxicol. Appl. Pharmacol., 329 (2017) 282-292.

[7] S. Pacey, M. Gore, D. Chao, U. Banerji, J. Larkin, S. Sarker, K. Owen, Y. Asad, F. Raynaud, M. Walton, A Phase II trial of 17-allylamino, 17-demethoxygeldanamycin (17-AAG, tanespimycin) in patients with metastatic melanoma, Invest. New Drugs, 30 (2012) 341-349.

[8] Q. Wei, J.-Y. Ning, X. Dai, Y.-D. Gao, L. Su, B.-X. Zhao, J.-Y. Miao, Discovery of novel HSP90 inhibitors that induced apoptosis and impaired autophagic flux in A549 lung cancer cells, Eur. J. Med. Chem., 145 (2018) 551-558.

[9] L. Shrestha, A. Bolaender, H. J Patel, T. Taldone, Heat Shock Protein (HSP) drug discovery and development: Targeting heat shock proteins in disease, Curr. Top. Med. Chem., 16 (2016) 2753-2764.

[10] J. Garcia, S. Barluenga, K. Gorska, F. Sasse, N. Winssinger, Synthesis of

deguelin–biotin conjugates and investigation into deguelin's interactions, Biorg. Med. Chem., 20 (2012) 672-680.

[11] S.H. Oh, J.K. Woo, Y.D. Yazici, J.N. Myers, W.-Y. Kim, Q. Jin, S.S. Hong, H.-J. Park, Y.-G. Suh, K.-W. Kim, Structural basis for depletion of heat shock protein 90 client proteins by deguelin, J. Natl. Cancer Inst., 99 (2007) 949-961.

[12] D.-J. Chang, H. An, K.-s. Kim, H.H. Kim, J. Jung, J.M. Lee, N.-J. Kim, Y.T. Han, H. Yun, S. Lee, Design, synthesis, and biological evaluation of novel deguelin-based heat shock protein 90 (HSP90) inhibitors targeting proliferation and angiogenesis, J. Med. Chem., 55 (2012) 10863-10884.

[13] S. Lee, H. An, D.-J. Chang, J. Jang, K. Kim, J. Sim, J. Lee, Y.-G. Suh, Total synthesis of (−)-deguelin via an iterative pyran-ring formation strategy, Chem. Commun., 51 (2015) 9026-9029.

[14] H. Yao, J. Liu, S. Xu, Z. Zhu, J. Xu, The structural modification of natural products for novel drug discovery, Expert Opin. Drug Discov., 12 (2017) 121-140.

[15] V.A. Steadman, S.B. Pettit, K.G. Poullennec, L. Lazarides, A.J. Keats, D.K. Dean, S.J. Stanway, C.A. Austin, J.A. Sanvoisin, G.M. Watt, Discovery of potent cyclophilin inhibitors based on the structural simplification of sanglifehrin A, J. Med. Chem., 60 (2017) 1000-1017.

[16] H.S. Kim, M. Hong, J. Ann, S. Yoon, C.-T. Nguyen, S.-C. Lee, H.-Y. Lee, Y.-G. Suh, J.H. Seo, H. Choi, Synthesis and biological evaluation of C-ring truncated deguelin derivatives as heat shock protein 90 (HSP90) inhibitors, Biorg. Med. Chem., 24 (2016) 6082-6093.

[17] H.S. Kim, M. Hong, S.-C. Lee, H.-Y. Lee, Y.-G. Suh, D.-C. Oh, J.H. Seo, H. Choi, J.Y. Kim, K.-W. Kim, Ring-truncated deguelin derivatives as potent Hypoxia Inducible Factor-1α (HIF-1α) inhibitors, Eur. J. Med. Chem., 104 (2015) 157-164.

[18] M. Nayak, I. Kim, Alkyne carbonyl metathesis as a means to make 4-acyl chromenes: syntheses of (±)-deguelin and (±)-munduserone, The Journal of organic chemistry, 80 (2015) 11460-11467.

[19] S. Xu, G. Wang, F. Xu, W. Li, A. Lin, H. Yao, J. Xu, Concise total synthesis of (±)-deguelin and (±)-tephrosin using a vinyl iodide as a key building block, J. Nat.

Prod., 81 (2018) 1055-1059.

[20] M. Wang, A. Shen, C. Zhang, Z. Song, J. Ai, H. Liu, L. Sun, J. Ding, M. Geng, A. Zhang, Development of heat shock protein (HSP90) inhibitors to combat resistance to tyrosine kinase inhibitors through HSP90–kinase interactions, J. Med. Chem., 59 (2016) 5563-5586.

[21] V. Thamilselvan, M. Menon, S. Thamilselvan, Anticancer efficacy of deguelin in human prostate cancer cells targeting glycogen synthase kinase- 3 β/β- catenin pathway, Int. J. Cancer, 129 (2011) 2916-2927.

[22] P. Pandya, J.L. Orgaz, V. Sanz- Moreno, Modes of invasion during tumour dissemination, Mol. Oncol., 11 (2017) 5-27.

[23] Y. Zhou, S. Li, J. Li, D. Wang, Q. Li, Effect of microRNA-135a on cell proliferation, migration, invasion, apoptosis and tumor angiogenesis through the IGF-1/PI3K/Akt signaling pathway in non-small cell lung cancer, Cell. Physiol. Biochem., 42 (2017) 1431-1446.

[24] H. Zhao, Y. Jiao, Z. Zhang, Deguelin inhibits the migration and invasion of lung cancer A549 and H460 cells via regulating actin cytoskeleton rearrangement, Int. J. Clin. Exp. Pathol., 8 (2015) 15582.